NANO-MECHANICAL PROPERTIES OF HEAT INACTIVATED *BACILLUS ANTHRACIS* AND *BACILLUS THURINGIENSIS* SPORES

THESIS

Jessica L. Poindexter, 2nd Lieutenant, USAF

AFIT/GAP/ENP/08-M07

DEPARTMENT OF THE AIR FORCE
AIR UNIVERSITY

AIR FORCE INSTITUTE OF TECHNOLOGY

Wright-Patterson Air Force Base, Ohio

APPROVED FOR PUBLIC RELEASE; DISTRIBUTION UNLIMITED

The views expressed in this thesis are those of the author and do not reflect the official policy or position of the United States Air Force, Department of Defense, or the United States Government.

AFIT/GAP/ENP/08-M07

NANO-MECHANICAL PROPERTIES OF HEAT INACTIVATED *BACILLUS ANTHRACIS* AND *BACILLUS THURINGIENSIS* SPORES

THESIS

Presented to the Faculty

Department of Engineering Physics

Graduate School of Engineering and Management

Air Force Institute of Technology

Air University

Air Education and Training Command

In Partial Fulfillment of the Requirements for the

Degree of Master of Science in Applied Physics

Jessica L. Poindexter, BS

2nd Lieutenant, USAF

March 2008

APPROVED FOR PUBLIC RELEASE; DISTRIBUTION UNLIMITED

AFIT/GAP/ENP/08-M07

NANO-MECHANICAL PROPERTIES OF HEAT INACTIVATED *BACILLUS ANTHRACIS* AND *BACILLUS THURINGIENSIS* SPORES

Jessica L. Poindexter, BS
2nd Lieutenant, USAF

Approved:

Larry W. Burggraf (Chairman) — 21 Mar 08 — Date

Charles A. Bleckmann (Member) — 21 Mar 08 — Date

Guangming Li (Member) — Mar 21, 2008 — Date

Abstract

B. thuringiensis has been proposed as a possible simulant for *B. anthracis* in counter-proliferation studies because it is closely related to *B. anthracis* and is not harmful to humans. In order to be a good simulant in counter-proliferation studies, *B. thuringiensis* spores must have similar properties to *B. anthracis* spores. In particular, they must behave in a similar way when exposed to high temperatures for short periods of time as would be caused by an explosion. This research examines the difference in surface elasticities of the spores of the two species and how exposure to heat just sufficient to inactivate the spores changes their elasticities. A method developed by Dr. Li at AFIT is used to measure the surface elasticities. This method measures the reflection and transmission of acoustic waves between the surface of the spore and the AFM tip to find the surface stiffness and then uses the Hertz contact model to determine the surface elasticity (Young's modulus). Surface elasticities were determined for four different sample types: *B. anthracis* spores, *B. thuringiensis* spores, heat inactivated *B. anthracis* spores, and heat inactivated *B. thuringiensis* spores. Measurements were taken on spores with AFM cantilevers of two different stiffnesses, 0.06 N/m and 0.58 N/m. The surface elasticities of the two spore species were different. Measurements using the tip with stiffness 0.58 N/m on *B. anthracis* gave average elasticity 3.73 GPa with standard deviation 0.22 GPa, and on *B. thuringiensis* average elasticity of 4.67 GPa with standard deviation 0.72 GPa. This indicates that *B. anthracis* has a structurally different outer spore coat layer than *B. thuringiensis*. Heat inactivation resulted in a decrease in spore surface elasticity. Measurements using the tip with stiffness 0.58 N/m on heat

inactivated *B. anthracis* spores gave average elasticity of 2.73 GPa with standard deviation of 0.29 GPa, and on heat inactivated *B. thuringiensis* spores of average elasticity 3.57 GPa with standard deviation 0.27 GPa. The elasticities were fairly uniform across the spore surface, even over features of varying height. The softer cantilever tip gave lower values of elasticity due to its interation with the adsorbed water layer on the spore surface and fragments of the exosporium.

Acknowledgments

I would first like to thank Dr. Li for teaching me how to use the AFM, answering all my questions on why it wasn't working, and helping me figure out what I was doing wrong.

I would like to thank Dr. Burggraf for his support and giving me an extension on my thesis when I realized I had to pretty much retake all my data at the beginning of January.

I would like to thank Major Hawkins for taking the time to help figure out appropriate heating time and temperatures for my samples and running them through the oven for me.

Thank you to Dr. Bleckmann for giving Major Hawkins and me an overview of the lab and safety procedures and answering my unending questions on what equipment, dyes, and chemicals the lab had.

I would also like to thank Dr. Felker for helping Major Hawkins and I find the equipment and supplies we needed in the labs, figure out how they worked and get them set up and running properly, and letting us know when the water wasn't working.

Table of Contents

Page

Abstract iv

Acknowledgements vi

Table of Contents vii

List of Figures ix

List of Tables xi

I. Introduction 1

Overview 1
Purpose of Research 2
Research Objectives 4
Scope and Limits of Research 4

II. Literature Review 6

Overview 6
B. anthracis versus *B. thuringiensis* 6
Spore Structure 8
Sporulation and Germination 11
Atomic Force Microscope (AFM) 15
AFM Used to Determine Spore Structure 16
Measuring Elasticity with the AFM 18

III. Methodology 21

Experimental Overview 21
Spore Growth and Preparation 21
Sample Preparation 23
AFM Technique 25

IV. Results and Analysis 32

Observations on Spore Growth, Harvesting, and Sample Preparation 32
Reflection Amplitude Curves 35

Page

Surface Features....36
Elasticity Results....38

V. Discussion....43

Overview....43
Assumptions Made in the Experimental Method....43
Linking Observations to Theory....44
Recommendations for Future Work....45
Conclusions....46

Appendix A. Suppliers....48

Appendix B. Elasticity Calculation....50

Appendix C. Spore Elasticity Data....53

Bibliography....63

List of Figures

Figure Page

1. Spore structure of group 1 bacilli....9
2. Spore coat folding....10
3. AFM images of germination in *B. atrophaeus*. 14
4. AFM design 16
5. AFM images of spore coat layers 18
6. *B. thuringiensis* sample mounted for AFM measurement 24
7. Diagram of the experimental setup of the AFM, LIA, Dual Channel Filter, and Signal Access Module 26
8. Photograph of the experimental setup including the AFM, Dual Channel Filter, and Signal Access Module 27
9. Photograph of the Lock-In Amplifiers....28
10. AFM height images of a *B. thuringiensis* spore showing data sampling scan line....30
11. AFM height images of spores with exosporia 33
12. AFM images of sonicated and non-sonicated spores....34
13. Curve fitting of reflectance amplitude for soft tip on *B. anthracis* spore 35
14. Curve fitting of reflectance amplitude for stiff tip on *B. anthracis* spore 35
15. AFM image of *B. thuringiensis* spore and sample point height cross sections with soft tip....36
16. AFM image of *B. thuringiensis* spore and sample point height cross sections with stiff tip 37

Figure Page

17. AFM image of *B. anthracis* spore and sample point height cross sections with soft tip 37

18. AFM image of *B. anthracis* spore and sample point height cross sections with stiff tip 38

19. Graph of mean elasticities of height feature points on spore samples measured with the stiff tip 41

20. Hertz Contact Model 51

21. *B. anthracis* spore 1 AFM image and elasticity graph 53

22. *B. anthracis* spore 2 AFM image and elasticity graph 54

23. *B. anthracis* spore 3 AFM image and elasticity graph 54

24. *B. anthracis* spore 4 AFM image and elasticity graph 55

25. Heated *B. anthracis* spore 1 AFM image and elasticity graph 56

26. Heated *B. anthracis* spore 2 AFM image and elasticity graph 56

27. Heated *B. anthracis* spore 3 AFM image and elasticity graph 57

28. Heated *B. anthracis* spore 4 AFM image and elasticity graph 57

29. Heated *B. anthracis* spore 5 AFM image and elasticity graph 58

30. *B. thuringiensis* spore 1 AFM image and elasticity graph 59

31. *B. thuringiensis* spore 2 AFM image and elasticity graph 59

32. *B. thuringiensis* spore 3 AFM image and elasticity graph 60

33. *B. thuringiensis* spore 4 AFM image and elasticity graph 60

34. *B. thuringiensis* spore 5 AFM image and elasticity graph 61

35. Heated *B. thuringiensis* spore 1 AFM image and elasticity graph 62

36. Heated *B. thuringiensis* spore 2 AFM image and elasticity graph 62

List of Tables

Table Page

1. Elasticity mean and standard deviation for spores with soft tip 39
2. Elasticity mean and standard deviation for spores with stiff tip 39
3. T-test 95% confidence interval of elasticity values for spore samples measured with stiff tip 40
4. T-test 95% confidence interval of elasticity values for spore samples measured with soft tip.....40
5. T-test 95% confidence interval of elasticity values for surface features in spore samples measured with stiff tip 42
6. Elasticity values for *B. anthracis* spore 1 taken with soft tip 53
7. Elasticity values for *B. anthracis* spore 2 taken with soft tip 54
8. Elasticity values for *B. anthracis* spore 3 taken with stiff tip 54
9. Elasticity values for *B. anthracis* spore 4 taken with stiff tip 55
10. Elasticity values for heat inactivated *B. anthracis* spore 1 taken with soft tip.....56
11. Elasticity values for heat inactivated *B. anthracis* spore 2 taken with stiff tip 56
12. Elasticity values for heat inactivated *B. anthracis* spore 3 taken with stiff tip 57
13. Elasticity values for heat inactivated *B. anthracis* spore 4 taken with stiff tip 57
14. Elasticity values for heat inactivated *B. anthracis* spore 5 taken with stiff tip 58
15. Elasticity values for *B. thuringiensis* spore 1 taken with soft tip.....59
16. Elasticity values for *B. thuringiensis* spore 2 taken with soft tip.....59

Table Page

17. Elasticity values for *B. thuringiensis* spore 3 taken with stiff tip 60

18. Elasticity values for *B. thuringiensis* spore 4 taken with stiff tip 60

19. Elasticity values for *B. thuringiensis* spore 5 taken with stiff tip 61

20. Elasticity values for heat inactivated *B. thuringiensis* spore 1 taken with soft tip 62

21. Elasticity values for heat inactivated *B. thuringiensis* spore 2 taken with stiff tip 62

NANO-MECHANICAL PROPERTIES OF HEAT INACTIVATED *BACILLUS ANTHRACIS* AND *BACILLUS THURINGIENSIS* SPORES

I. Introduction

Overview

Bacterial spores are unique biological entities. Bacteria form them in times of stress when their environment is no longer favorable for continued replication due to lack of nutrients, extreme temperatures, toxic substances, or other factors. The bacterial spore preserves the bacteria's genetic information until a time when the environment is again favorable for growth and replication.

Bacterial spores are of special interest to the government because of their potential use as biological weapons. *Bacillus anthracis*, the causative agent of the disease anthrax, is the primary spore-producing bacterial species of interest. Anthrax is a zoonosis, typically infecting cattle, sheep, and goats, but capable of crossing over to humans. It is naturally a soil dwelling organism and causes cutaneous infections when the spores infect cuts or breaks in the skin. However, it can also cause a pulmonary infection if the spores are inhaled as sometimes happens when working with wool or hides. The weaponized form of the spores is an aerosol designed to promote penetration into the lungs.

The possibility of anthrax being a threat as a bioweapon became reality in 2001 when terrorists sent spores in a powdered form in letters to two senators and several news media offices, killing five people and infecting 17 others (2001 anthrax attacks, 2007).

Since the anthrax bacteria is easy to grow and weaponize, it is important that means are developed to counter such weapons. It is essential to have a good simulant bacteria to use in tests for counter-proliferation effects. The simulant needs to be a spore forming bacteria that closely resembles anthrax and reacts in a similar way to its environment, but poses no threat of disease or illness.

AFNWCA, the sponsor for this research, has chosen *Bacillus thuringiensis* as a possible simulant. *B. thuringiensis* and *B. anthracis* are very closely related differing by only a couple of plasmids and a few DNA sequences (Dwyer and others, 2004:23). They are so closely related that some have proposed that rather than being different species they are really two different strains of the same species (Radnedge and others, 2003:2755).

Purpose of Research

The purpose of this research project is to compare the material properties of *B. anthracis* and *B. thuringiensis* spores and to determine how their spore surface properties change when they are inactivated (killed) by heat. AFNWCA, the sponsor of this research, would like to use *B. thuringiensis* as a simulant for *B. anthracis* in studies of spore response to methods of deactivation in an effort to develop a model to accurately predict the neutralization of a bio-weapon stockpile in a counterforce strike. Knowledge of how the spores differ structurally and how their properties change after heat inactivation will lead to a better model for predicting *B. anthracis* spore neutrilization from data collected in studies using *B. thuringiensis* spores.

This research project will build on previous work at AFIT done by Captain Ruth Zolock and Dr. Guanming Li. Captain Zolock used the atomic force microscope (AFM)

to analyze the surface morphologies of *Bacillus* spores looking for identifiable features that could be used to distinguish four *Bacillus* species (Zolock, 2002:1; Zolock and others, 2006:363-369). Captain Zolock determined that there were no absolute surface morphology differences between the four strains studied that could be used to identify individual spores. However, populations of spores of different species and accurately identified by comparing the statistical distributions of spore surface features and AFM phase data (Zolock and others, 2006:368). Also different species varied in adhesion to substrates as observed previously by others. Both the overall surface features and adhesion are properties linked to the spore coat indicating that the spore coats should be different between species and possess different elastic characteristics.

The surface elasticities of the spores were determined using a method developed by Dr. Li at AFIT (Li and others, 2007:1). This method utilizes measurements of the reflection and transmission of acoustic waves between the AFM tip and the surface of the material. The near-surface stiffness of the interface is determined from the slope of the reflection amplitude. The elastic modulus is then determined from this using the Hertz contact model.

Heat inactivated spores were spores that had been exposed to a high temperature for time periods of a minute or less so that none of the spores were able to germinate. This was the total kill point, and was determined by Major Leslie Hawkins in her MS thesis *Micro-etched platforms for thermal inactivation of Bacillus anthracis and Bacillus thuringiensis spores*.

Research Objectives

The overall goal of this research project was to sompare the surface elasticities of *B. anthracis* and *B. thuringiensis* spores. More specifically I planned to address three aspects using elasticity measurements:

(1) Look for differences in bulk elasticities between the two species
   - Is there an identifiable difference?
   - Can the spores be distinguished based on this property?

(2) Determine if elasticity is uniform over the spore surface or whether it changes with surface contour.
   - Are there identifiable surface features with different elasticities?
   - How do these vary between *B. anthracis* and *B. thuringiensis*?

(3) How does heating to the point of spore inactivation change the elasticity of the spore surfaces?

Scope and Limits of Research

This research project only examined the surface elasticities of *B. anthracis* and *B. thuringiensis* spores. Only one temperature and time for heat inactivation was examined for each spore species. This was 160^{o} C for 45 seconds for *B. anthracis* and 140^{o} C for 60 seconds for *B. thuringiensis*. These temperatures and times were determined by Major Hawkins as the point where no spores grown and prepared by the methods used in my research were observed to germinate (Hawkins, 2008:53,54). Data was gathered on only five *B. anthracis* spores, five heat treated *B. anthracis* spores, five *B. thuringiensis*

spores, and two heat treated *B. thuringiensis* spores. Only two different AFM cantilever stiffnesses were used in taking measurements on the spores, 0.06 N/m and 0.58 N/m.

II. Literature Review

Overview

Although the government and military would like to better understand the *B. anthracis* organism, it is not always used in research. Often another organism is substituted that can be assumed to be similar, but is safer to work with. *B. subtilus* is the most often used model for the genus *Bacillus* because it is nonpathogenic, is common and easy to obtain, and has long been considered the standard model for the *Bacillus* genome. Consequently much of the information currently available on spores, how they are formed, and how they return to the active vegetative form of the cell is from research on this organism. More recently studies have been conducted to determine the differences in spores and spore formation for other *Bacillus* species including *B. cereus*, *B. thuringiensis*, and *B. anthracis*. *B. cereus* and *B. thuringiensis* are often used as a substitute for *B. anthracis* because they are very closely related to it, differing from it and each other by a couple of plasmids, a couple of genes for cell wall proteins, and several bacteriophage related sequences (Dwyer and others, 2004:23).

B. anthracis versus *B. thuringiensis*

All members of the genus *Bacillus* are gram-positive, aerobic, endospore forming, rod shaped bacteria. *B. anthracis* and *B. thuringiensis* belong to the group 1 bacilli, which also includes *B. cereus*. All members of the group 1 bacilli are closely related genetically, close enough that some researchers have proposed that they could be considered one species (Radnedge and others, 2003:2755).

The group 1 bacilli have specialized to become animal pathogens. *B. anthracis* is the causative agent of the disease anthrax. *B. thuringiensis* is often used in pesticides and bioengineering pest resistant crops because of its ability to produce an insecticidal parasporal crystal at the same time it forms its spore. *B. cereus* causes food poisoning and skin infection in humans. All three species are easily isolated from soil environments where their spores can exist for years.

Different characteristics were developed by the group 1 bacilli as they diverged genetically through rndom mutations and exchanging DNA with other soil organisms. Traditionally it has been thought that while in the soil, *Bacillus* organisms remain in their dormant spore form. Recent research has shown this is not always true. Paul C. Hanna of the University of Michigan Medical School has reported work where he has observed all stages of the *B. anthracis* lifecycle in soil (Pobojewski, 2004; Miller, 2004:142). This activity indicates that the organism could exchange genes with related bacteria or pick them up from phages in the soil. Such gene exchanges can change the nature of an organism to help it adapt to its environment, enabling it to exhibit virulence characteristics or antibiotic resistance (Schuch and Fischetti, 2006:3037). At least three proteins that are part of the *B. anthracis* spore surface structure come from phages (Stone, 2006:309; Schuch and Fischetti, 2006:3049).

The disease anthrax is a result of the expression of genes on two plasmids in *B. anthracis.* One plasmid codes for the synthesis of a capsule around the bacterial cell and the other codes for three toxin proteins (Thorne, 1993:115). The *B. anthracis* strain used in this research was the Sterne strain which originally came from an attenuated *B. anthracis* strain isolated by M. Sterne in 1937 (Koehler, 2000:526). The Sterne strain

does not produce a capsule around vegetative cells since the pXO2 plasmid is missing. It has been used as a vaccine since its isolation, and is still currently used by veterinarians. However, it still has a low level of virulence in some animals since the bacteria are capable of producing the toxins (Koehler, 2000:526).

Spore Structure

Bacterial spores are hardy, resistant, dormant structures that bacteria form in reaction to unfavorable environmental conditions. Spores allow bacteria to preserve genetic material until environmental conditions are again favorable to support growth and division. Spores have no metabolic activity, exchange no enzymes or other macromolecules with their environment, low water activity, DNA immobilization, low enzyme activity, and no active DNA repair (Moir, 2006:526; Liu and others, 2004:164). Since no DNA repair occurs in the spore, damage accumulates over time. If this damage is extensive enough, the spore won't be able to complete germination.

The bacterial spore consists of several protein and lipid layers surrounding a central core containing the nuclear material, ribosomes, and cytoplasm. A diagram of the spore structure for *B. anthracis* and *B. thuringiensis* is shown in Figure 1.

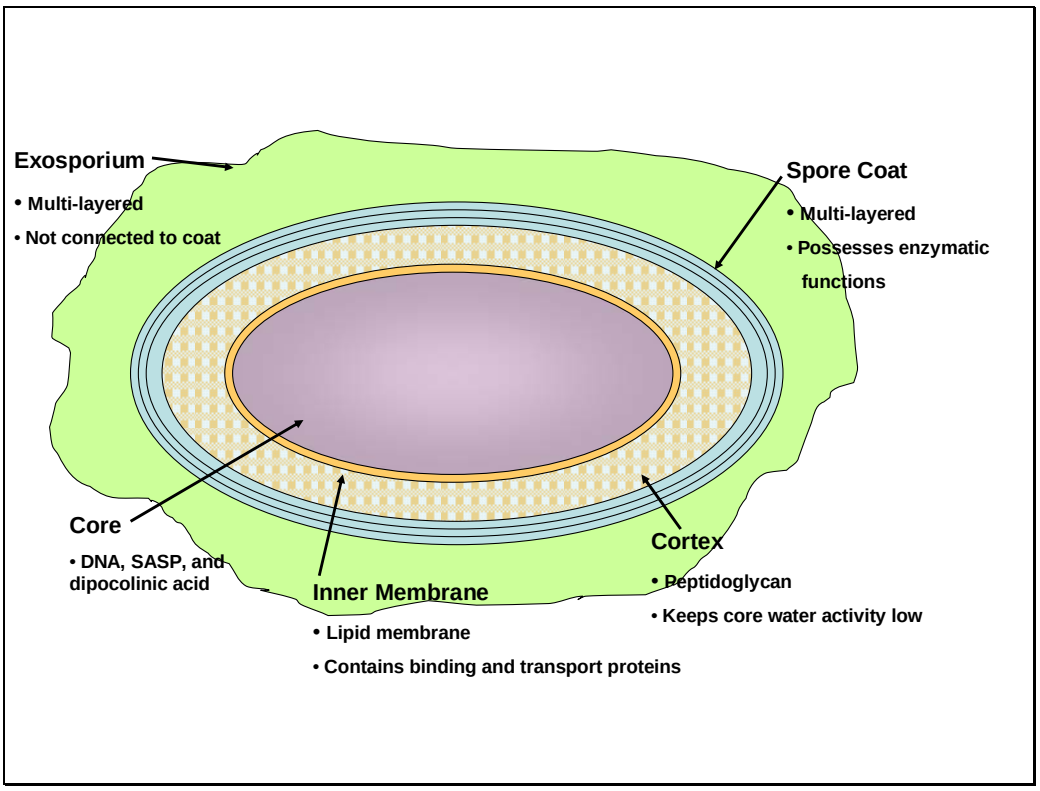

Figure 1. Spore structure of group 1 bacilli.

The outermost layer of the spore is composed of a loose membrane called the exosporium that forms an envelope around the spore and can be easily removed. Electromicrographs of the exosporium in *B. anthracis* indicate that it has an outer layer composed of fine filamentous structures about 720 Å in length and 100 Å in diameter (Hachisuka, Kojima and Sato, 1966:2382). Underneath is a basal membrane roughly 90 to 110 Å thick (Gerhardt, 1964:1780). The function of the exosporium is unknown although its absence does not change the virulence of the organism (Giorno and others, 2007:701) or the ability of the spore to germinate.

The next layer is the spore coat. The exosporium and spore coat are a separated by a space called the interspace (Giorno and others, 2007:691). It is unknown what the interspace consists of though it has been hypothesized that it is compressible with spring-

like properties since the distance the exosporium is from the spore coat can vary greatly (Giorno and others, 2007:699).

The spore coat of *B. anthracis* has two distinct layers when viewed in electron micrographs (Giorno and others, 2007:691). The function of the spore coat is to act as a sieve to molecules entering the spore. Defects in the spore coat lead to a higher rate of germination since more molecules triggering the process can enter the spore (Giorno and others, 2007:702).

The spore coat is attached to the underlying spore cortex. As the spore cortex and core shrink due to dehydration the spore coat folds to form ridges along its length as shown in Figure 2. The thickness of the coat can vary depending on the medium the organism is grown in (Driks, 1999:6).

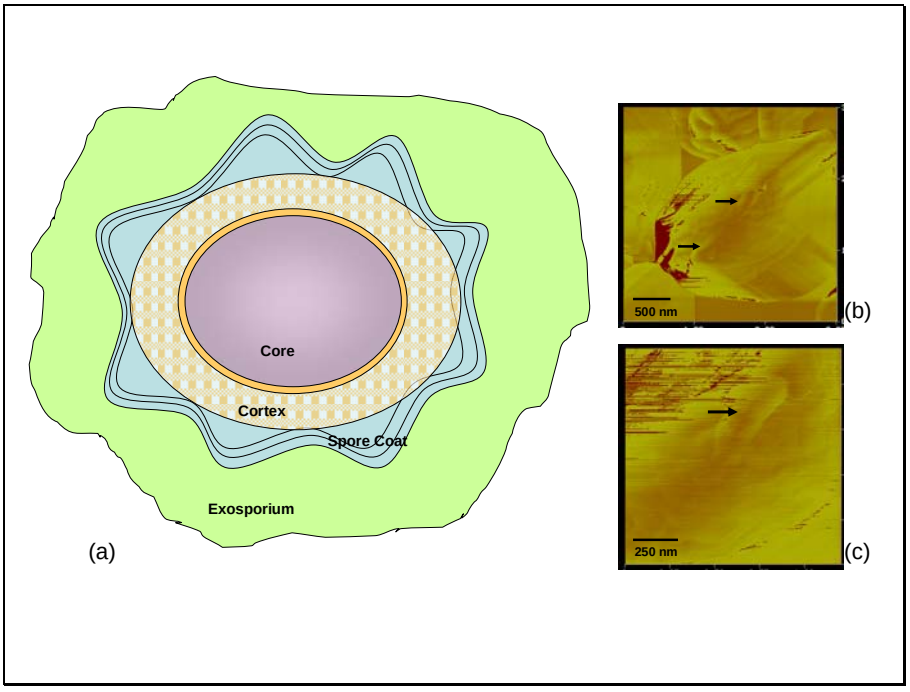

Figure 2. Spore coat folding. (a) Diagram of cross section of spore. (b) AFM contact mode height image of *B. thuringiensis* spore showing ridges along the surface from spore coat folding, indicated by black arrows. (b) Closer image of ridge.

The spore cortex is composed of peptidoglycan, similar to the protein forming the walls of vegetative cells. However, peptidoglycan in spores differs from peptidoglycan in cell walls in cross-linking and composition (Driks, 2004:1249). The cortex helps keep the core water activity low.

The last layer around the spore core is the inner membrane. In order to trigger the germination of a spore, a germinant (such as an amino acid, sugar, or nucleoside) must interact with proteins embedded in this inner membrane (Moir, 2006:526).

The core of the spore is where the organism's DNA is stored and protected by surrounding it with dipocolinic acid and small acid soluble proteins (SASP). Recent work has used SASPs as biomarkers to differentiate between *B. anthracis* and *B. cereus*, as well as determine phylogenetic relationships between strains (Castanha and others, 2007:199).

Sporulation and Germination

Sporulation is the process where a vegetative cell produces a spore due to unfavorable environmental conditions like a lack of nutrients. Germination in the process the spore goes through to transform back into an active vegetative cell. As the spore begins the process of germination it becomes more vulnerable to its environment. Studies on germination have revealed a better understanding of spore structure and the roles played by each of the layers.

Germination is composed of three stages, activation, germination, and outgrowth (Moberly and others, 1966:221). In the first stage, activation, the germinant passes through the exosporium, spore coat, and cortex, to interact with and probably bind with a

receptor protein in the inner membrane. This results in an increase in the fluidity of the inner membrane (Moir and others, 2002:403).

Spore germination is triggered by environmental factors such as the presence of a nutrient, change in temperature, or change in pressure. The nutrient may be a simple amino acid, sugar or nucleoside (Moir, 2006:526) and differs from species to species. The presence of more than one germinant nutrient may be required to initiate germination. Adenosine, L-alanine, DL-tyrosine have been used to trigger germination in *B. anthracis* (Moberly, Shafa, and Gerhardt, 1966:220).

Moir, Corfe, and Behrahven identified a family of receptor proteins, ion transporter enzymes, and core lytic enzymes produced by *Bacillus* species that are involved in the process of germination. Germination can also be induced chemically by calcium dipicolinate. However, this may involve a different germination process than is induced by the presence of a nutrient or may appear different because the germination process is started at a later step (Moir and others, 2002:407).

The second stage of germination is called germination. During this stage the spore begins to release calcium ions and dipicolinate into its environment and take up water. Ion fluxes between the interior of the spore and its surrounding environment resume as monovalent cations move across the inner membrane (Moir and others, 2002:403). The spore cortex and spore coat are degraded. Since the spore can't build molecules to break down the spore coat and cortex, it is believed that these molecules are produced during sporulation by the mother cell and embedded in the spore coat, cortex, or in between them (Plomp and others, 2007:9646).

Although some of the genes and proteins involved in the germination process have been identified, the molecular details of the signal process in the spore during germination are still unclear. It is unknown how the enzyme that breaks down the cortex of the spore is activated (Moir, 2006:529).

The final stage in the germination process is outgrowth. In this stage, the vegetative cell emerges from the protective layers of the cortex and spore coat, and begins division. Metabolism is resumed, and any DNA damage is repaired. Any macromolecules needed in the germination process must already be present in the spore since no bulk transport or metabolism occurs until after outgrowth (Moir, 2006:526). Until outgrowth, the processes processes in germination will proceed regardless of the extent of damage to the DNA since they are independent from the spore's DNA. If the DNA has been damaged beyond repair, the new cell that emerges in outgrowth won't be able to function and will die.

Although the exact molecular process in germination is still unclear, research done with the atomic force microscope (AFM) has helped shed more light on the structural basis of germination. Researchers have used the AFM to study the germination process in *B. atrophaeus,* which from further research seems to have a similar external spore structure to *B. cereus* (Plomp and others, 2005b:604). Both *B. cereus* and *B. atrophaeus* have an outer spore coat layer composed of crystalline parallel rodlets (Plomp and others, 2007:9645). The AFM was used to image spores through the entire process of germination as the outer rodlet layer was broken down and the vegetative cell eventually emerged from the cortex.

The process began with the formation of 2-3 nm pits in the rodlet layer that the researchers guessed were formed by hydrolytic enzymes. They hypothesized that these enzymes were located in the spore integument and activated in the early stages of germination (Plomp and others, 2007:9646). These enzymes could be localized where the pits formed. Another possibility they suggested was that the pits could form at point defects in the rodlet structure. The pits eventually connected to form fissures in the outer layer of the spore. As time progressed, these fissures widened, lengthened, and eventually coalesced. They became apertures that grew, until they were big enough that the vegetative cell could emerge. AFM images of germination in a *B. atrophaeus* spore are shown below in Figure 3.

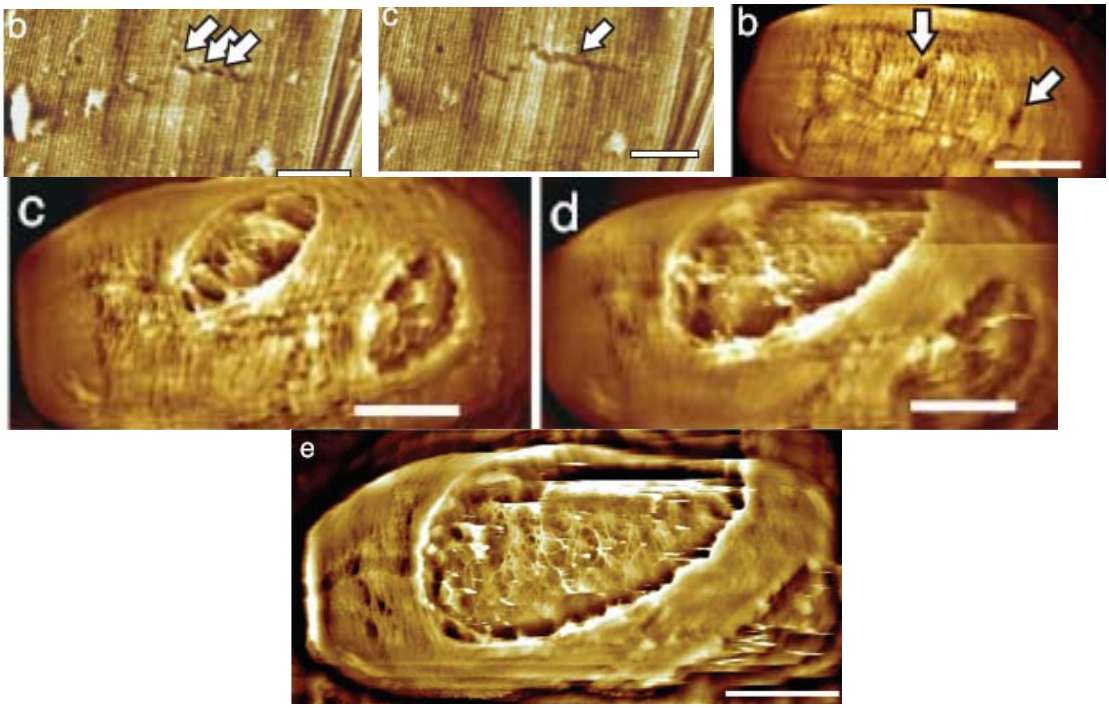

(Plomp and others, 2007:9645,9647)

Figure 3. AFM images of germination in *B. atrophaeus*.

Although the *B. atrophaeus* spore structure seems to share some physical similarities to *B. cereus*, *B. thuringiensis* has no outer rodlet layer. Since both *B. cereus*

and *B. thuringiensis* are closely related to *B. anthracis*, *B. anthracis* could have a structure similar to one or the other. No work has yet been done to identify the molecular structure and appearance of *B. anthracis'* outer spore coat layers. The process for the breakdown of the outer layers of the spore and the emergence of the vegetative cell most likely follows a similar process.

Atomic Force Microscope (AFM)

The atomic force microscope (AFM) has been growing in importance as a tool in microbiology since its invention in 1986. It is unique since it allows atomic scale resolution of biological materials without a lot of preparation. Cells can even be imaged as they go through their life cycle. Recently the AFM has been used to examine the structure of *Bacillus* spores as well as examine mechanical properties of biological substances including cells, cell walls, and spores.

The AFM was developed in 1986 by Binning, Quate, and Gerber in a collaboration between IBM and Stanford University. It produces topological images of surfaces. Minimal preparation is needed for samples in comparison to light and electron microscopy samples, and they can be observed in real time under physiological conditions (Dufrêne, 2007:96). Images are created by sensing the force between a sharp probe tip and the sample surface. The sample is mounted on a piezoelectric scanner that can move the sample in the x, y, and z directions to insure the probe tip remains in contact with the surface, while the sample is moved back and forth to allow the probe tip to scan over it.

The probe tip is attached to a soft cantilever whose deflection is measured to determine the force between the tip and the sample surface. A laser beam is focused on

the end of the cantilever where the probe tip is, and reflected to a photodiode. Changes in the position of the laser beam determine the deflection of the cantilever. A feedback circuit keeps the piezocrystal adjusting height to maintain a certain deflection in the cantilever and a constant force between the tip and sample. A diagram of the AFM design is shown in Figure 3.

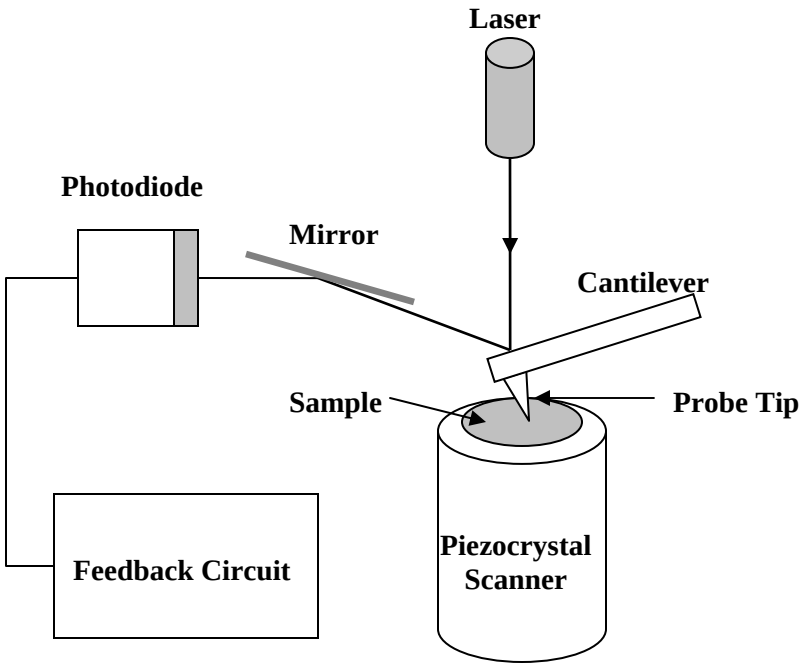

Figure 4. AFM design.

AFM Used to Determine Spore Structure

Captain Zolock used the AFM to analyze the surface morphologies of *Bacillus* spores looking for identifiable features that could be used to distinguish between four *Bacillus* species (Zolock, 2002:1; Zolock and others, 2006:363-369). She analyzed spores from *Bacillus anthracis* Sterne strain, *Bacillus thuringiensis* var. *kurstaki*, *Bacillus*

cereus strain 569, and *Bacillus globigii* var. *niger*. Zolock determined that there were no absolute surface morphology differences between the four strains studied that could be used to identify them. However, populations of spores of different species were distinguished by comparing the statistical distributions of spore surface features and AFM phase data (Zolock and others, 2006:368).

Phase images in AFM are a result of surface-tip interactions and surface visco-elasticity. The phase lags can be influenced by variations in a material's surface properties such as adhesion, friction, visco-elasticity, and stiffness. Areas that are less elastic tend to appear brighter in the image. Zolock and others were able to conclude that although there were no large surface features making a spore immediately identifiable, the surface properties did vary significantly between species.

Other studies have also used the AFM to characterize spore morphologies and look for identifiable differences between spores of different species. Zaman and others used the AFM to look at size changes as B. anthracis spores germinated in conjunction with a transmission electron microscope (TEM) to observe internal changes in the spores (Zaman and others, 2005:307).

The AFM has also been used to compare morphological features of the spore surface and first inner layer of the spore coat of *B. cereus*, *B. thuringiensis*, and *B. atrophaeus*. The researchers removed the exosporium and the first outer layer of the spore coat by sonication. They were able to see structural differences in the spore coat layers of the three species with a significant difference in the first spore coat layer between *B. cereus* and *B. thuringiensis* as shown in Figure 4 (Plomp and others, 2005b:605). These researchers also determined that the species specific spore surface

structural variations between *B. cereus* and *B. thuringiensis* correlated to differences in gene sequences for the spore core structural protein SspE (Plomp and others, 2005a:7893).

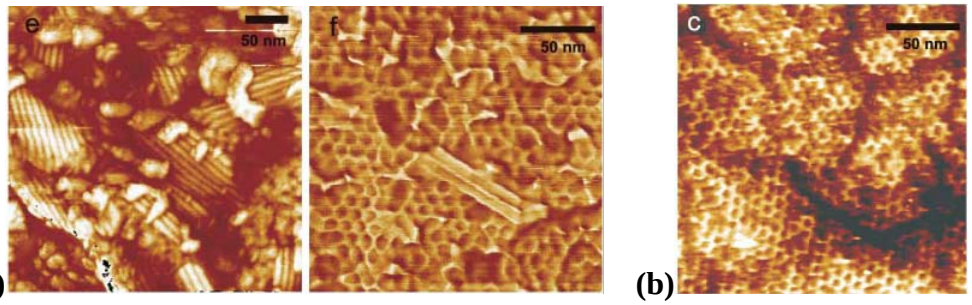

(a) **(b)**

(Plomp and others, 2005a:7896)

Figure 5. AFM images of spore coat layers. (a) *B. cereus*, showing an outer layer composed of patches of rodlets overlaying a layer with honeycomb structure. (b) *B. thuringiensis*, with the spore coat composed of a honeycomb structure. There is no rodlet layer.

Plomp and others also examined changes in spore surface morphology due to hydration. Spores in 65% relative humidity decreased to 88% the size of those in water (Plomp and others, 2005b:606). Air drying resulted in ridges along the spore surface that the researchers concluded were due to the spore coat folding as the core shrunk in size due to dehydration. They decided that this demonstrated that the spore coat itself didn't shrink or expand as Driks had proposed, but was flexible enough to compensate for changes in the internal volume of the spore by surface folding (Plomp and others, 2005b:606).

Measuring Elasticity with the AFM

There are two techniques that have been commonly used to measure the elasticities of surfaces of biological materials with the AFM. The first is the indentation method. In this method, the probe tip is pressed into the sample surface and then pulled

off while the force versus distance of the probe from the surface is recorded. Since biological materials are soft and deformable, a reference force curve must first be recorded for a hard sample. The difference between the curves for the reference material and the biological sample give the deformation of the biological sample under the tip load (Vinckier and Semenza, 1998:13). This is then plotted against the force to create a force-versus-indentation curve. The elasticity (Young's modulus) can be determined using this graph and the geometry of the probe tip.

The second method to measure elasticities in biological materials is called the "depression technique" (Dufrene, 2007:104). In this method the part of the biological specimen that the elasticity is to be measured for, such as an organelle or cell wall components, is separated from the whole cell and placed on a hard substrate and allowed to dry. The AFM probe tip is placed on the sample and the force is increased and decreased while the deflection of the cantilever is measured. Comparisons between the deflections for the soft sample and the hard substrate allow the elastic modulus to be determined for the material.

Lateral variations in elasticity have been determined by creating spatially resolved force maps (A-Hassan and others, 1998:1564). In this method, arrays of force versus distance curves are recorded at the same time as topographic images. The same method is applied as in the indentation method to determine the elastic modulus for these points.

These methods contain a high amount of error and uncertainty due to the difficulty of tip calibration, poorly defined contact geometry, depth of penetration, piezocreep, hysteresis effects, and fitting the force curves to the Hertz model (A-Hassan, 1998:1565; Li and others, 2007:2). The method developed by Dr. Li at AFIT avoids

some of these pitfalls by making use of acoustic reflections between the tip and the surface of the material being measured (Li and others, 2007:1). Unlike with the other methods, the interactions between the tip and surface do not need to be explicitly defined with this method. The measurements of the acoustic reflections give the near-surface stiffness for the material. The elastic modulus is determined from this by using a simple contact mechanics model. The calculations for this method are given in Appendix B.

The AFM has been used to measure the surface elasticities of a variety of microbial organisms including *Pseudomonas putida*, *Bacillus subtilis*, *Aspergillus nidulans* spores, *Magnetospirillum gryphiwaldense*, and *Methanospirillum hungatei*. However, no studies have yet been performed on *B. anthracis*, or either of its two closest genetic relatives *B. cereus* and *B. thuringiensis*.

III. Methodology

Experimental Overview

Since this research built on previous work done by Captain Ruth Zolock using the AFM to characterize *Bacillus* spores, I used similar microbiological techniques except where available supplies limited me or other literature sources indicated simpler and quicker methods. This research also used the acoustic technique developed by Dr. Guangming Li to use the AFM to measure elasticities of spore surfaces. *B. thuringiensis* and *B. anthracis* cultures were grown on beef extract agar in petri dishes. After completing sporulation, the spores were removed from the plates, cleaned in three centrifuge washes, and then droplets of spore suspension were deposited on a graphite substrate. A lock-in amplifier was used to send a signal into the piezocrystal of the AFM while running the cantilever over the spore surface. The reflection and transmission of this signal through the piezocrystal was measured and analyzed to determine the surface elasticities.

Spore Growth and Preparation

Sterilization was done in a Tuttnaur Brinkmann 3870 autoclave. When media was prepared and water sterilized it was autoclaved at 121^{o} C at 15 psi for 15 minutes steam. Liquid waste and used pipette tips were autoclaved at 121^{o} C at 20 psi for 15 minutes steam and 20 minutes dry. All pipette tips and petri dishes used came from pre-sterilized packages. All spores were grown in plastic petri dishes on Criterion Dehydrated Culture Media, which contained per liter of formula 15 grams agar, 5 grams gelatin peptone, and 3 grams beef extract.

The source of the Bacteria used in this research came from Dr. Eric Holwitt of the Air Force Research Laboratories, Biomechanisms and Modeling Branch, Brooks Air Force Base, Texas. The bacteria were supplied as lyophilized spores stored in glass culture tubes, in a locked cabinet, at room temperature. The *B. thuringiensis* strain used (variant kurstaki) was isolated by Brooks researchers from a commercially available insecticide Javelin® (Ortho® brand, no longer manufactured). The safety standard for handling this organism is BioSafety Level 1 organism. The *B. anthracis* strain used was the Sterne strain and came from a veterinary, nonencapsulated, live culture of the anthrax spore vaccine. The safety standard for handling this organism is Biosafety Level 2 organism (Zolock, 2002:65). All manipulation of the spores was conducted in a Napco Class II Type A/B3 Biosafety Cabinet.

Initial cultures were grown by streaking two plates from the lyophilized *B. anthracis* spore sample and two plates from the lyophilized *B. thuringiensis* sample. All further growth was taken from streaks made from these 4 plates. The plates were incubated at 37^{o} C in an incubator. After 4 days of growth it became apparent that the *B. anthracis* plates were contaminated with a phage. Care was taken to select phage free areas to streak two new plates. The new *B. anthracis* plates showed no signs of phage infection. All plates were placed in the refrigerator at 4^{o} C after 7 days of growth. Further plates were streaked from these original plates as needed. A quick check for sporulation was made by Gram staining before spores were harvested from the plates and by using phase contrast microscopy.

The following technique was used to harvest the spores. Sterile water was pipetted onto the culture plate until the entire surface was covered. The water was mixed

in with the bacterial growth using a glass spread rod while care was taken not to gouge the agar. A fresh pipette was used to pipette the slurry of the surface of the plate into two plastic centrifuge tubes. More sterile water was added to the tubes to bring their volumes to 1/3 full (about 5 mL). The tubes were capped and vortexed to mix thoroughly and break up clumps of bacteria and spores. Then the tubes were centrifuged at 4000 rpm (3200g) for 20 min at 4^{o} C in a Eppendorf Centrifuge 5810R. Literature research indicated that spores should be centrifuged at 10000g for 10 min to separate spores from cellular debris (Nicholson and Setlow, 1990:415). However this was not possible with the centrifuge available in the lab. After centrifuging, the supernatant was poured off, fresh sterile water was added to bring the volume of the tube to 5 mL, and the contents were thoroughly mixed by vortexing. This process was repeated twice more so that the spore samples were centrifuged three times. The final spore solution was checked by Gram staining to determine whether any cellular debris was present and if further washes were needed and then was stored at 4^{o} C.

Sample Preparation

Spore samples were deposited onto a graphite substrate that was mounted on a 15 mm steel disc. Two samples of HOPG (highly ordered pyrolytic graphite) were used to prepare the substrate. One was 12 x 12 mm and the other 10 x 10 mm. The 10 x 10 mm size was easiest to work with. The HOPG blocks were split into four sections with an x-acto blade. Each section was than affixed to a steel disk using a sticky tab. After this, cellophane tape was used to cleave the graphite to provide a clean smooth surface. A pipette was used to mix the spore solution and then deposit a droplet about 5 mm in diameter on the graphite surface. The droplet was allowed to sit undisturbed for 5

minutes and then rinsed off with cold sterile water. During the 5 minutes, spores settled out of the solution and adhered to the graphite. The sample was allowed to dry and then stored in a petri dish in a drawer at room temperature. Three samples of *B. thuringiensis* spores were prepared. One was heat treated by Major Hawkins in a ceramic heater at 140^{o} C for 60 seconds, one was prepared from a sonicated spore solution, and one was prepared from just a plain spore solution. Two samples of *B. anthracis* were prepared. One was the untreated spore solution and the other was heat treated by Major Hawkins in a Vulcan Box Furnace 3-130 at 160^{o} C for 45 seconds. Times and temperatures for heat treatment were determined by Major Hawkins as the threshold point where all spores were killed. At this point the spores had sustained enough damage that they could not germinate.

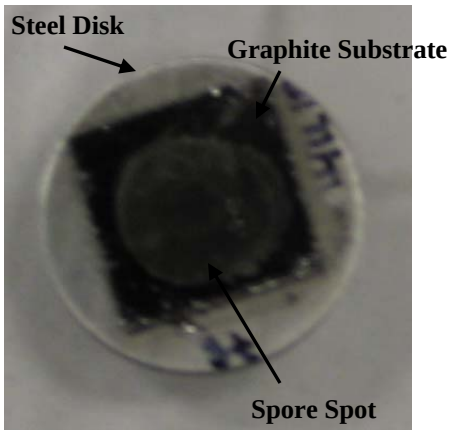

Figure 6: *B. thuringiensis* sample mounted for AFM measurement.

The sonicated sample was prepared in an effort to removed the spore exosporium and compare how this affected surface elasticity values. To prepare the sonicated sample, 500 μL of spore solution was pipetted into a fresh sterile centrifuge tube. The tube was suspended in a water bath in a Cole-Parmer® Ultrasonic Cleaner Model 8890 and sonicated for about 20 seconds. Then it was placed in the refrigerator at 4^{o} C to cool

for several minutes. This was repeated 15 times with 20 minute cooling sessions after every 5 sonication trials. The cooling was necessary because the sonicator could not cool the water bath and sonication tends to heat the sample. Heat is one of the triggers that can lead to spore germination.

AFM Technique

The AFM technique I used followed the technique developed by Dr. Li in "Nanometer-Scale Elastic Modulus of Surfaces and Thin Films determined using an Atomic Force Microscope." The AFM used was a Nanoscope® IIIa Scanning Probe Microscope with a Nanoscope® Optical Viewing System. A low frequency signal supplied by a Stanford Research Systems SR850 lock-in amplifier (LIA) was sent into the Digital Instruments Signal Access Module for the AFM and applied to the piezocrystal signal labeled as Bias. The piezocrystal would try to correct for this added "noise." Part of the signal was transmitted through the piezocrystal and part was reflected back to the signal from the cantilever.

The low frequency signal sent to the AFM was first passed through a SR650 dual channel filter where the signal was chopped at 1.0 Hz and 1.05 kHz and its output gain was amplified to 10 dB. This signal was sent into the AFM piezocrystal and into a second LIA to serve as a base signal. The signal from the cantilever (reflection), labeled as In 0 on the Signal Access Module, and from the piezocrystal (transmission), labeled as LV Z, were each sent to one of the LIA where their phase lag and amplitude changes were recorded as the input frequency was varied from 1000 Hz to 1 Hz. A diagram of the experimental setup is shown in Figure 6 below. Figures 7 and 8 show photographs of the setup.

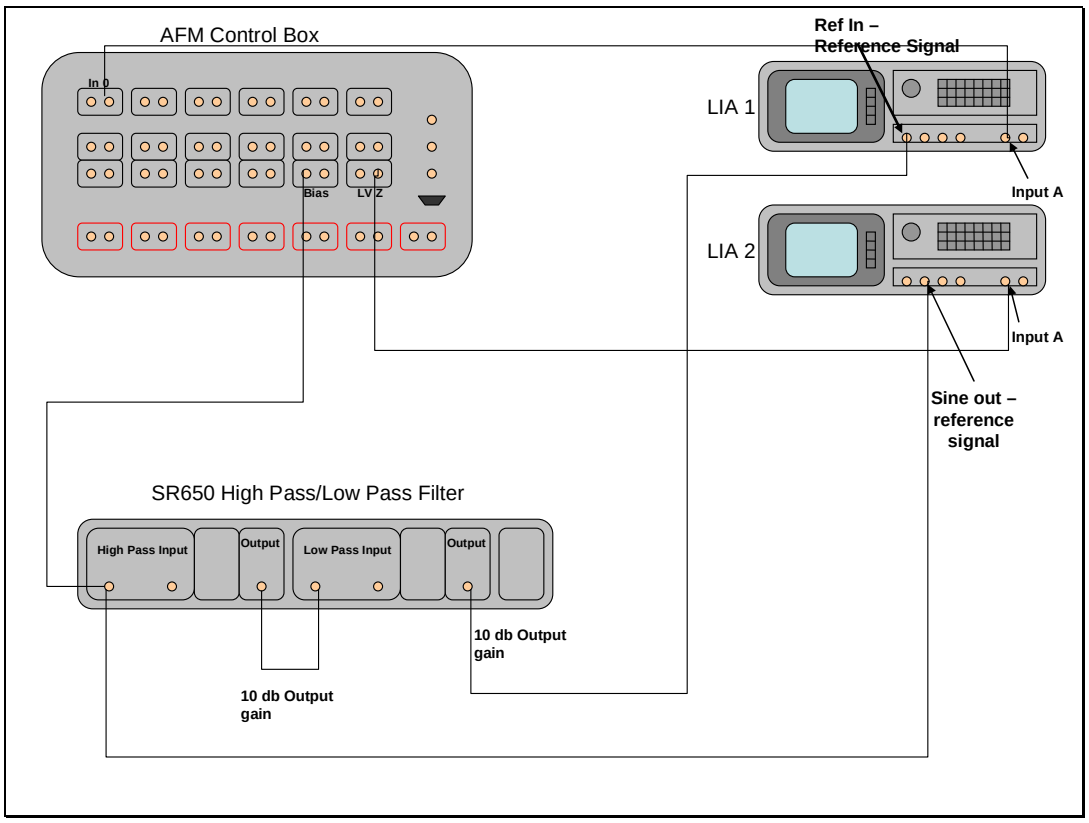

Figure 7. Diagram of the experimental setup of the AFM, LIA, Dual Channel Filter, and Signal Access Module.

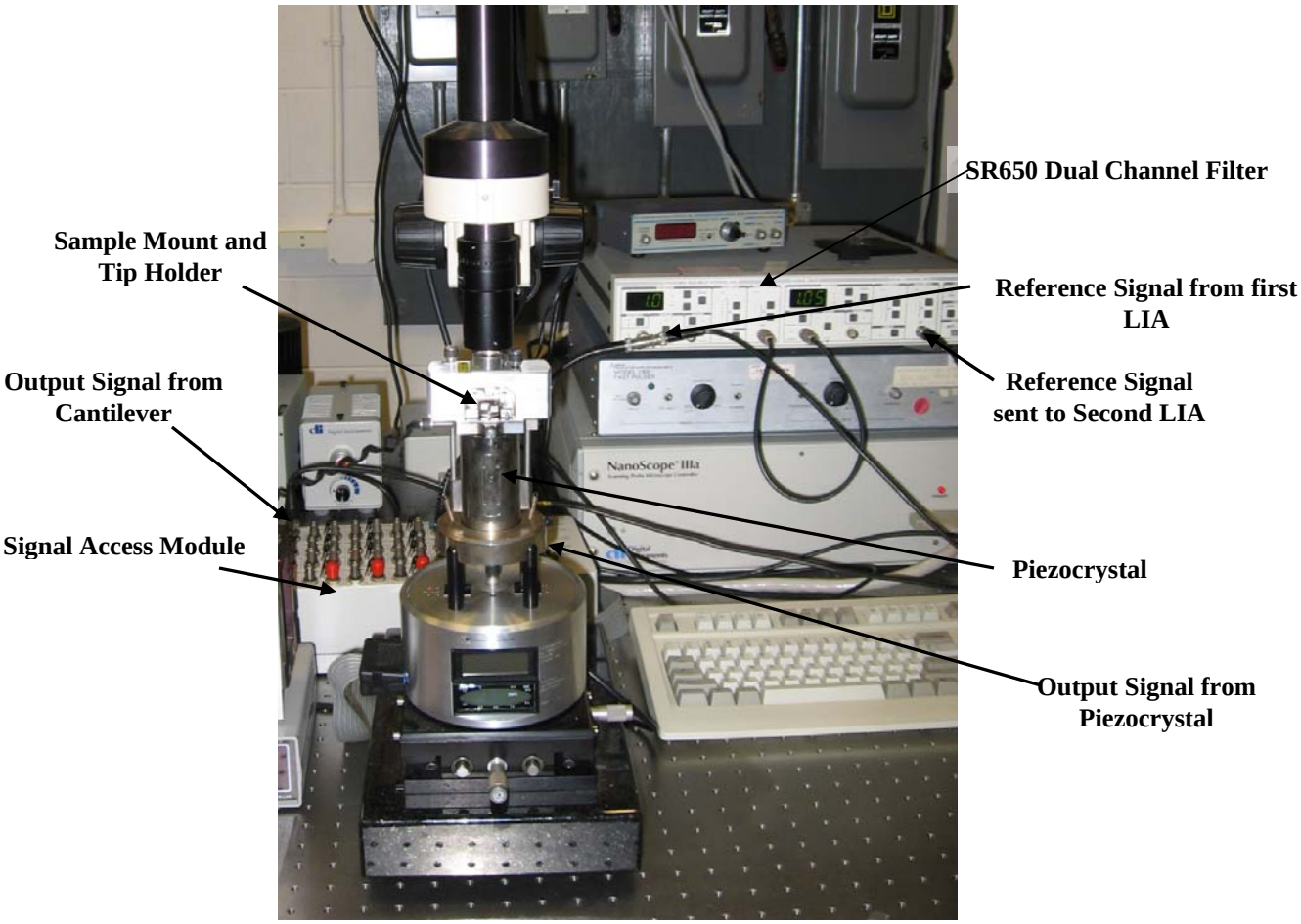

Figure 8: Photograph of the experimental setup including AFM, Dual Channel Filter and Signal Access Module.

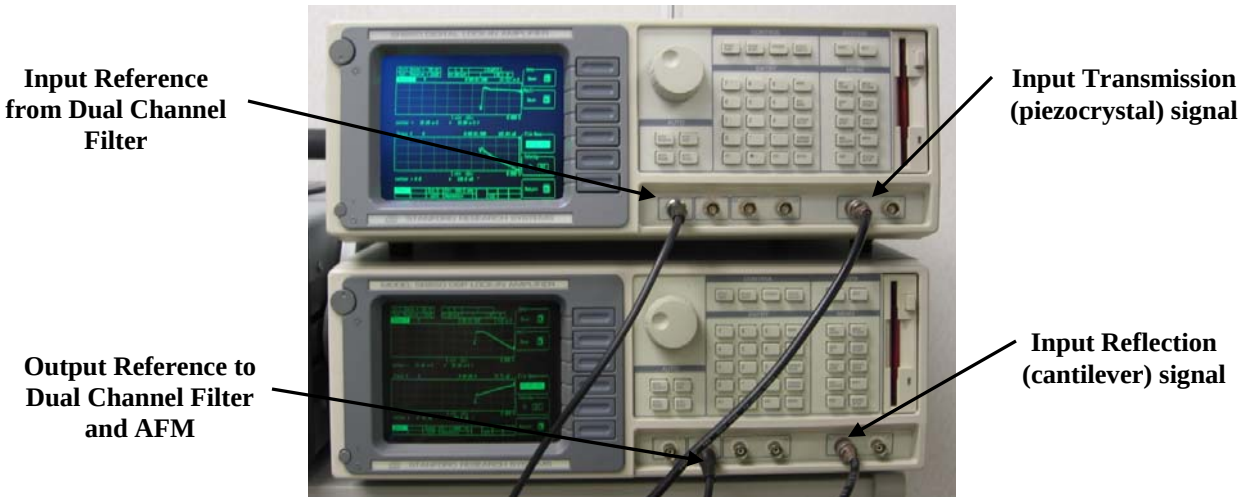

Figure 9: Photograph of Lock-In Amplifiers. The top LIA displays the transmissions (piezocrystal) data, and the bottom LIA displays reflection (cantilever) data. The top curve displayed on the LIA screen is amplitude and the bottom curve is phase lag.

To take data for a spore it was first necessary to find a spore. This was done by placing a spore sample in the AFM holder, loading the cantilever with the desired stiffness, and then taking an image in contact mode. An area of 6 μm x 6 μm was scanned at a rate of 2 Hz. Typically several spores would appear in this area. The AFM Zoom In feature was used to center on the selected spore. Trace and retrace images of the spore were recorded as I used the AFM to zoom in on the spore several times until I was scanning an area of about 500 nm x 500 nm roughly in the center of the spore. The scan was disabled when the scan line passed over an area of interesting features. Then I used the scope trace, which shows a vertical height cross section of the sample, to determine surface features and position the tip over either a ridge or a dip. Once this was done, I reduced the scan area to 1 nm, taking care to maintain tip position over the desired feature. Scan Rate was increased to 5.09 Hz. The deflection set point was set at 0 V, scan angle at 0^{o}, integral gain to 2, proportional gain to 3, and then the view mode

was changed to Force Calibration. The switch was flipped on the control box to allow the input signal from the LIA into the AFM. The force value in the top LCD display on the AFM was checked and adjusted to about -1.0 V using the top left knob.

Then I returned to image mode, and the x and y position coordinates were noted. The LIA start buttons were pressed at the same time to start recording the signals from the AFM. Three traces were taken, then the LIAs were stopped, the input signal was turned off and the scan length adjusted to 500 nm to choose a new feature to take a measurement of. Once the tip was moved to the new feature by using the arrow keys to adjust the x coordinates, the same procedure was followed. Usually five features (three traces each) were measured on each spore. A diagram showing the steps in focusing in on a spore, establishing a scan line, and then taking measurements at different points is shown in Figure 9 below.

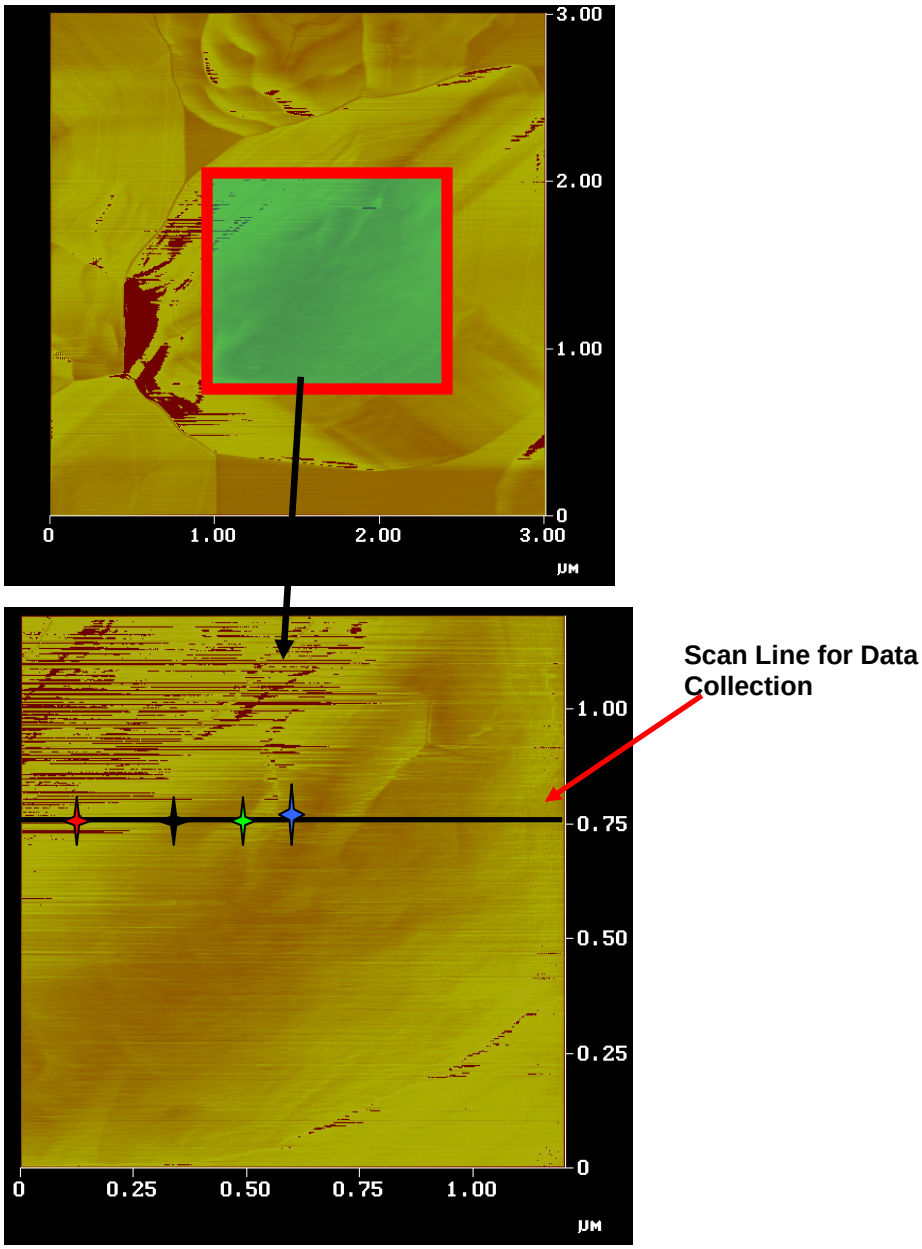

Figure 10: AFM height images of *B. thuringiensis* spore showing data sampling scan line. The red square indicates the zoomed in area shown in the bottom scan. The black line across the bottom scan shows where the scan was disabled on the spore surface and the stars indicate points with different height features where data was collected. For instance the blue star is on top of a ridge and the green star is in the dip beside the ridge.

Tips of two different stiffnesses were used to take the measurements. These tips were produced by Veeco Probes and had stiffnesses of 0.06 N/m and 0.58 N/m.

Elasticity values for spores were determined by comparing reflection amplitudes for the

spore samples with reflection amplitudes for HOPG graphite and a polystyrene sample, which had known elasticities. These elasticities had been previously determined by Dr. Li in his paper as 33 GPa for graphite and 2.5 to 3.5 GPa for polystyrene (Li and Burggraf, 2007:8). I used an average value of 3 GPa for the polystyrene. A different tip of each of the two stiffnesses was used for each type of spore sample. Tips were cleaned after taking measurements on two spores and before taking measurements on the polystyrene and graphite by rinsing with acetone for 30 seconds. The polystyrene sample had a molecular weight of 2,000,000 and a thickness of 160 to 220 nm.

To calculate the elasticities, a comparison was made between the known elasticities of the reference sample and the unknown elasticity of the spore sample by taking the ratio of the slopes of the reflection amplitudes for the reference and the spore. The slope of the reflection amplitude is inversely proportion to interfacial stiffness. Siffnesses are directly proportional to elasticity and by taking their ratio the unknown elasticity could be determined. The exact equations and calculations are detailed in Appendix B.

IV. Results and Analysis

Observations on Spore Growth, Harvesting and Sample Preparation

The two plates of *B. anthracis* that were streaked directly from the lyophilized spore sample had phage contamination that showed up as plaques on the bacterial growth. This may have been an outside contamination since previous work in the lab was done on soil samples or it may have simply been a lysogenic phage in the *B. anthracis* sample. Lysogeny is one of the methods of viral reproduction. The phage's genetic material is integrated into the host bacterium's genetic material and then passed on to daughter cells during division. The viral genetic material, called a prophage, can remain inactive in the cell until a late event, like UV radiation, causes it to activate and force the cell to produce new viruses and then lyse. I was able to isolate samples from regions of growth that weren't infected with the phage yet, and all further streak plates of *B. anthracis* were free of the lytic phage.

Although I centrifuged my spore samples at lower speed then recommended, my final preparation had little extra debris in it and no vegetative cells that I noticed when doing checks under a light microscope.

After sonication, I originally thought that I had destroyed all spores. But a spread plate made of the sonicated spore solution rapidly grew a bacterial lawn, indicating I still had a very high spore concentration in the solution. The images of the spores under the AFM appeared shorter than the nonsonicated samples.

Sonication didn't appear to remove the exosporrium anymore than it was in the nonsonicated sample. The exosporium was still present in a few cases. In the future it would be better to use a sonication probe since this can deliver a more direct hit of energy

directly to the sample rather than having to pass through the plastic wall of the container. This would also allow the removal of the first layer of the spore coat so the properties of the second layer could be examined.

In most of the spores examined the exosporium was partly removed and appeared fragmented as a result of the centrifuge washes. I was unable, however to clearly determine whether the the exosporium lay over the scan areas. Images of the sonicated spores, nonsonicated spores, and spores with and without exosporium are shown below in Figure 10 and Figure 11.

For preparing the samples I found it was easiest to use steel disks that were 15 mm in diameter and graphite that was 10 mm x 10 mm. Letting the spore solution sit on the graphite for 5 minutes gave a nice, even covering of spores.

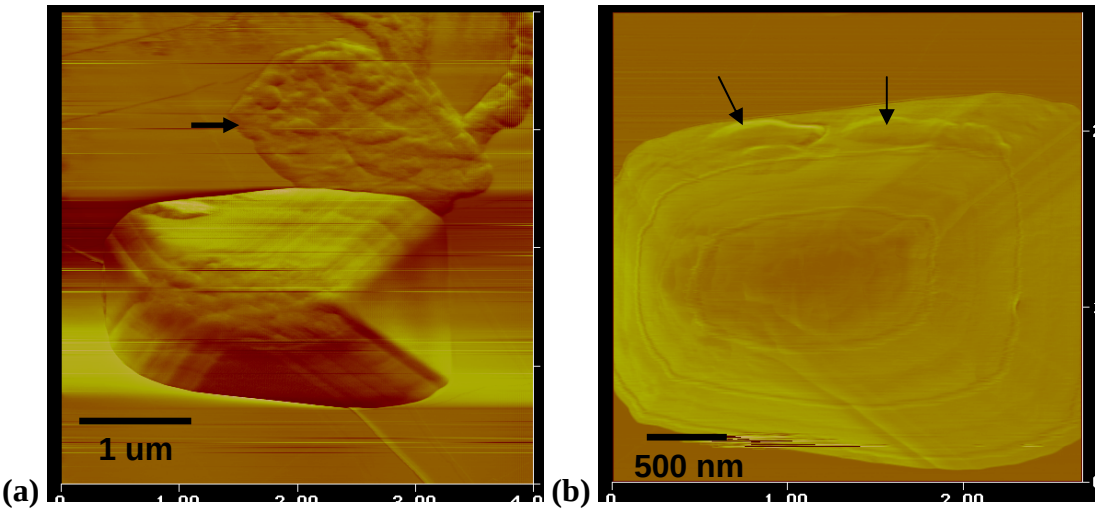

Figure 11. AFM height images of spores with exosporia. (a) *B. thuringiensis* spore. Black arrow indicates the exosporium that has partially come loose from the spore. (b) *B. anthracis* spore. Arrow indicates ripples that are likely from fragments of the exosporium still attached to the spore coat.

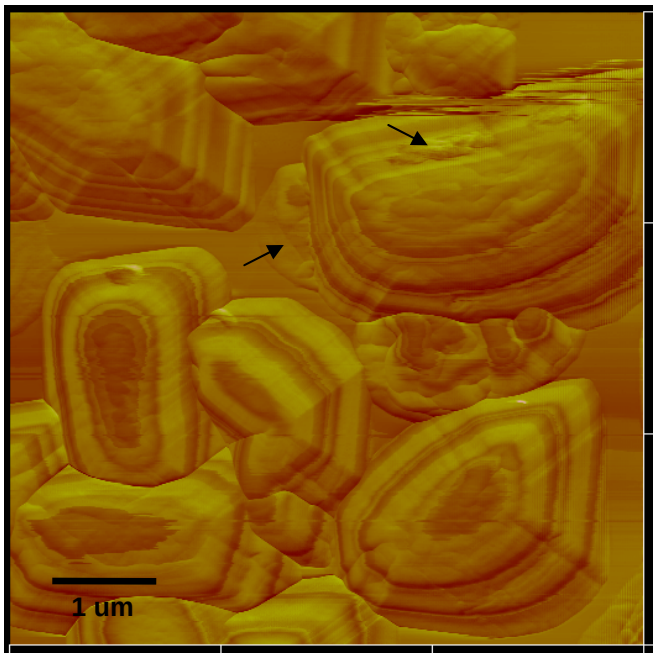

(a)

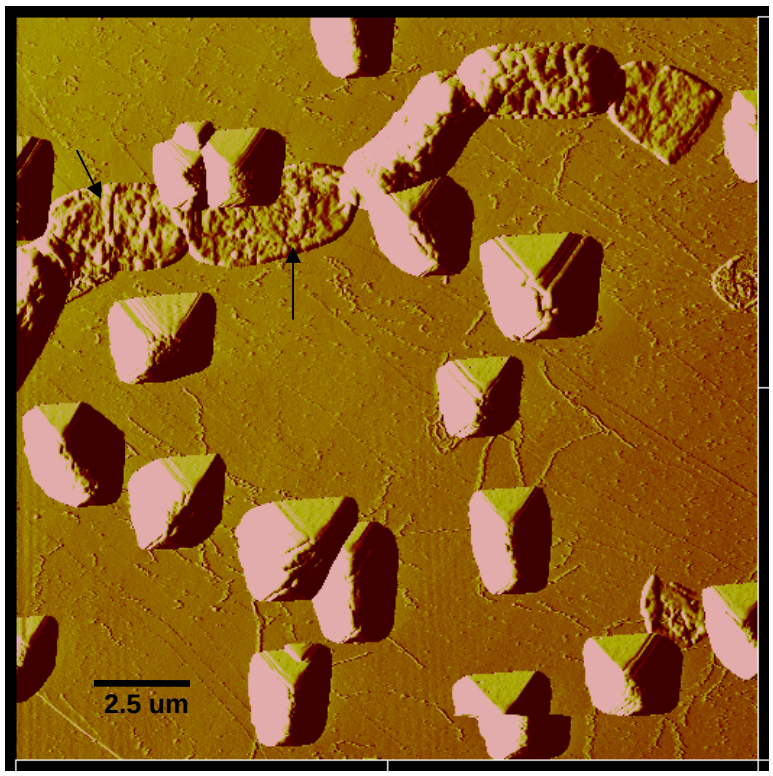

(b)

Figure 12. AFM images of sonicated and non-sonicated spores. (a) *B. thuringiensis* spores that have not been sonicated. (b) Sonicated *B. thuringiensis* spores. Arrows indicate exosporia.

Reflection Amplitude Curves

The reflection amplitude curves for data taken with the softer tip often had a sharp peak in the middle of the data which made curve fitting difficult. An example of this is shown below in Figure 12. Figure 13 shows the reflection amplitude curve taken with a stiffer tip. The reflection amplitudes taken with stiffer tips were always smooth curves as shown in Figure 13 and never exhibited the peaks that commonly showed up between about 200 and 500 Hz for softer tips. This behavior is probably due to the effects of adsorbed water on the surface of the spore. The softer tip would get stuck in the water layer, while the stiffer tip would push through it.

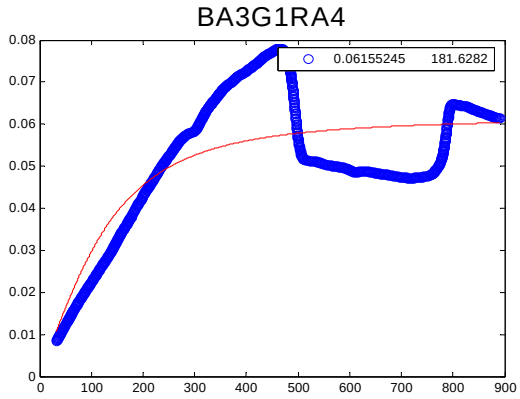

Figure 13. Curve Fitting of Reflectance Amplitude for soft tip on *B. anthracis* spore.

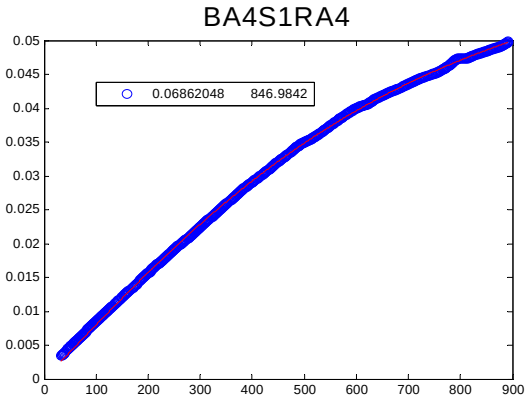

Figure 14. Curve Fitting of Reflectance Amplitude for stiff tip on *B. anthracis* spore.

Surface Features

The surface features I examined were ridges and valleys that appeared in the height cross section of the scan. The majority were about 3 to 5 nm in height or depth, and these corresponded to the rough rippled texture on the spore surface. Not all spores had large ridges in their coats running lengthwise. When they did, these were often 6 to 12 nm in height. There was not a great difference in the calculated elasticities between these surface features. Examples of scan cross sections and the spores they come from are shown below. The only spore in the images below that has a ridge due to spore coat folding is in Figure 14. As can be seen in Figure 15, it was occasionally difficult to find very many surface features of varying height. Some spore height cross section scan lines were relatively flat with often only one height feature along them.

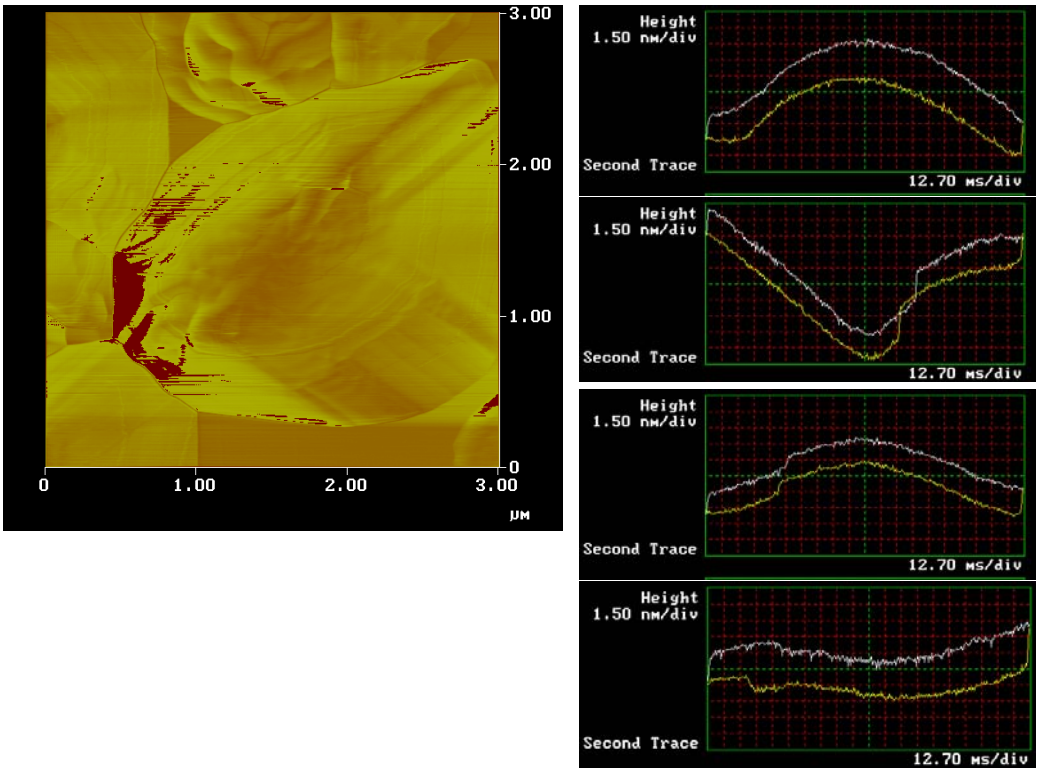

Figure 15. AFM image of *B. thuringiensis* spore and sample point height cross sections with soft tip.

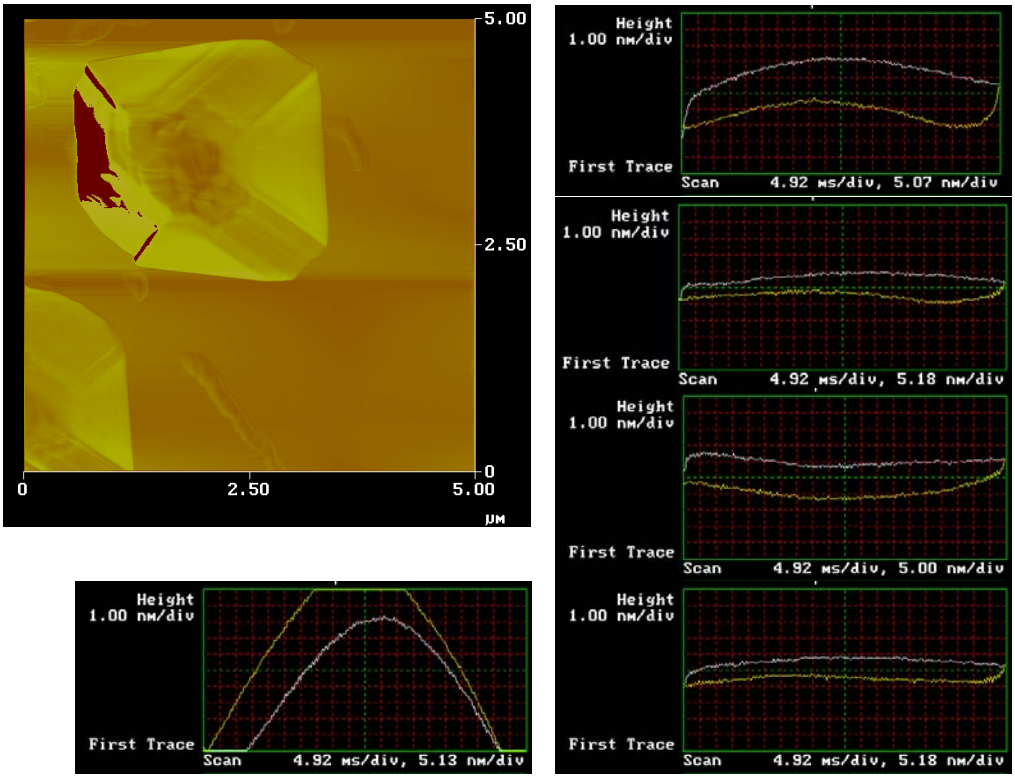

Figure 16. AFM image of *B. thuringiensis* spore and sample point height cross sections with stiff tip.

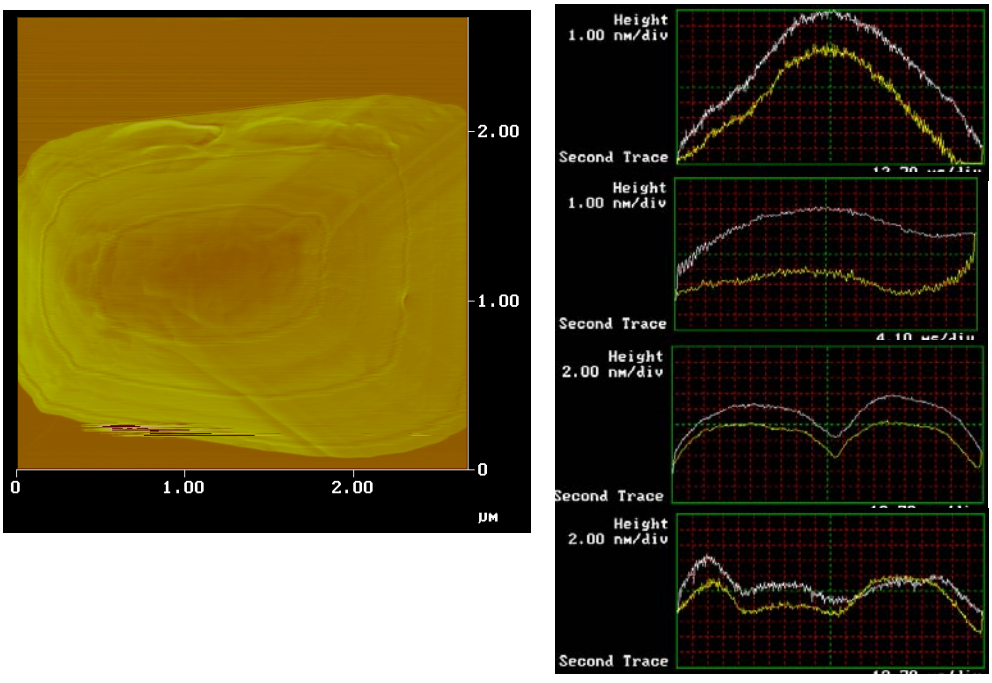

Figure 17. AFM image of *B. anthracis* spore and sample point height cross sections with soft tip.

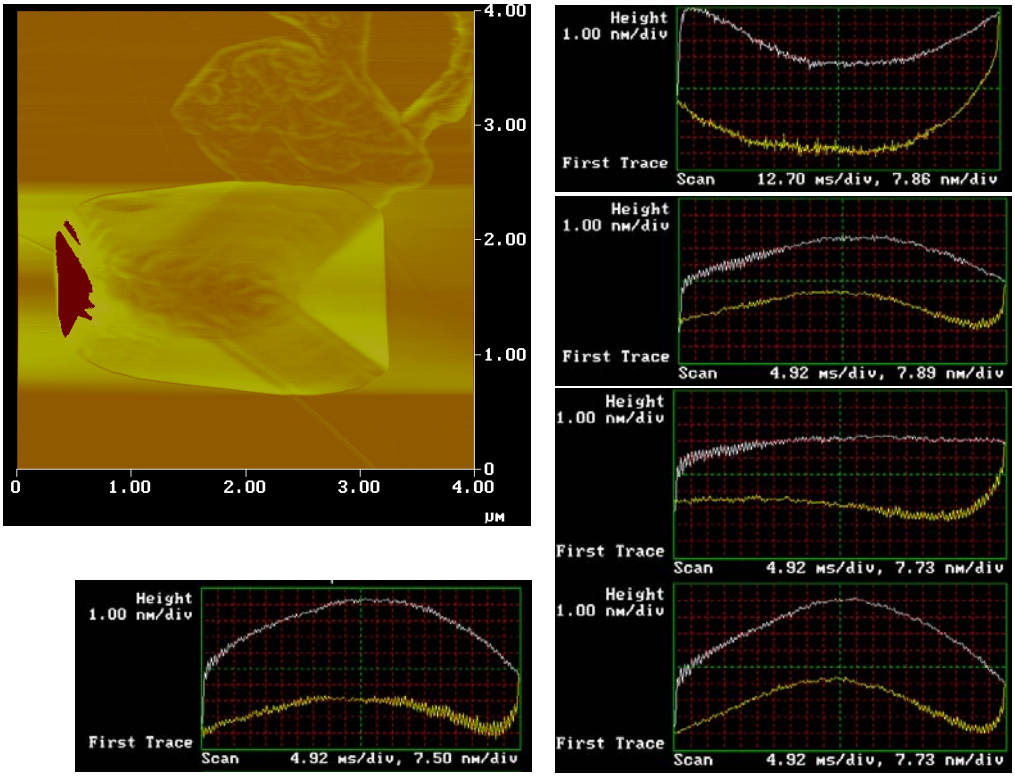

Figure 18. AFM image of *B. anthracis* spore and sample point height cross sections with stiff tip.

Elasticity Results

Four to five points were sampled across the scan line along a spore surface, the particular feature of the point was noted, and the elasticities calculated. Measurements were made for four types of spore samples: *B. thuringiensis* spores, *B. anthracis* spores, heat inactivated *B. thuringiensis* spores, and heat inactivated *B. anthracis* spores. The sonicated *B. thuringiensis* spores were not measured due to time constraints and because it was unclear whether the exosporium had been successfully removed. Measurements were taken on spores with cantilevers of two different stiffnesses. The soft cantilever had a stiffness of 0.06 N/m and the stiff cantilever had a stiffness of 0.58 N/m. Table 1 and Table 2 below show the overall means and standard deviations of calculated surface elasticity for each type of spore sample measured with the soft tip and the stiff tip.

Table 1. Elasticity mean and standard deviation for spores measured with soft tip.

Name	Mean elasticity (GPa)	Standard Deviation
B. anthracis	1.98	0.66
Heat Inactivated *B. anthracis*	1.31	0.22
B. thuringiensis	1.15	0.28
Heat Inactivated *B. thuringiensis*	3.74	3.61

Table 2. Elasticity mean and standard deviation for spores measured with stiff tip.

Name	Mean elasticity (GPa)	Standard Deviation
B. anthracis	3.73	0.22
Heat Inactivated *B. anthracis*	2.73	0.29
B. thuringiensis	4.67	0.72
Heat Inactivated *B. thuringiensis*	3.57	0.27

Heating the spores reduced their surface elasticity. Measured with the stiff tip, the *B. anthracis* spores had an average elasticity of 3.73 GPa. The heat inactivated *B. anthracis* spores had an average elasticity of 2.73 GPa. Similar behavior is seen in the *B. thuringiensis* spores. The *B. thuringiensis* spores had an average elasticity of 4.67 GPa. The heat inactivated *B. thuringiensis* spores had an average elasticity of 3.57 GPa. Using a Student's T-test with 95% confidence confirms that the mean elasticities of the heat inactivated spores are significantly different from those that were not heat inactivated, as well as the fact that *B. anthracis* and *B. thuringiensis* spores differ significantly in surface elasticity values. Table 3 below gives the 95% confidence intervals of mean elasticity for the spore samples measured with a stiff tip.

Table 3. T-test 95% confidence interval of elasticity values for spore samples measured with stiff tip.

Name	95% confidence interval of mean elasticity in GPa	
B. anthracis	3.629	3.823
Heat inactivated *B. anthracis*	2.647	2.805
B. thuringiensis	4.438	4.898
Heat inactivated *B. thuringiensis*	3.419	3.717

The soft tips gave smaller values for elasticity than the stiff tips. I presume this is due to the interaction of the soft tip with the adsorbed water layer on the surface of the spore. A soft tip would only interact with the very outmost layer of the spore, probably the outermost fragmented layer of the exosporium or the adsorbed water layer. The stiff tips would be able to push through the water layer and measure the elasticity of the layers of the spore surface underneath. Using a t-test to compare the mean elasticities for the soft tip results confirmed that they were significantly different from those measured by the stiff tips as well as from each other. Table 4 gives the 95% confidence intervals of mean elasticity values for the samples measured with soft tips.

Table 4. T-test 95% confidence interval of elasticity values for spore samples measured with soft tip.

Name	95% confidence interval of mean elasticity in GPa	
B. anthracis	1.668	2.437
Heat inactivated *B. anthracis*	1.185	1.426
B. thuringiensis	0.995	1.266
Heat inactivated *B. thuringiensis*	1.818	5.663

Three different height features were observable during measurements, ridge, dip, and flat. Using the t-test to compare the mean elasticities of the surface features in samples over a 95% confidence interval confirmed that they did not vary significantly from each other. They don't follow a regular pattern with ridge elasticity varying in a predictable way from dip elasticity. Figure 18 below shows a graph depicting the mean elasticity values calculated for each surface feature measured in the spore samples. Table 5 gives the 95% confidence interval for the mean elasticity values for the three different observed surface features in each type of spore sample.

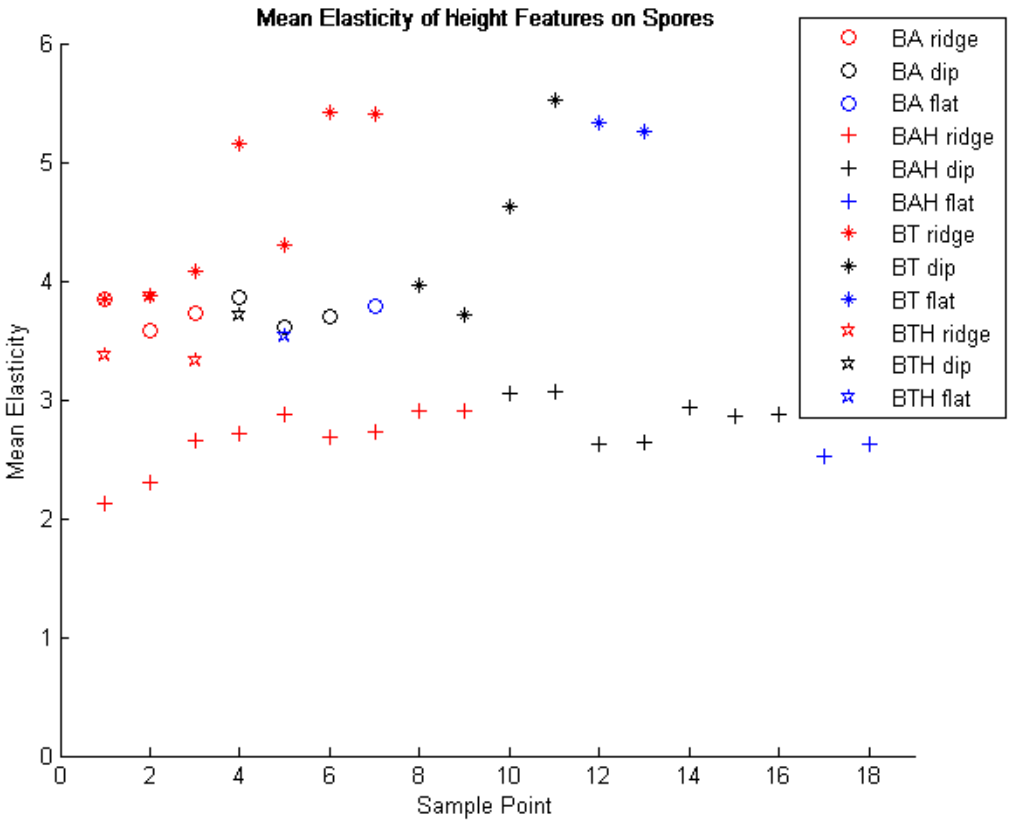

Figure 19. Graph of mean elasticities of height feature points on spore samples measured with the stiff tip.

Table 5. T-test 95% confidence interval of elasticity values for surface features in spore samples measured with stiff tip.

Sample and feature	**95% confidence interval in GPa**	
B. anthracis ridge	3.561	3.878
B. anthracis dip	3.601	3.826
B. anthracis flat	2.639	4.931
Heated *B. anthracis* ridge	2.535	2.774
Heated *B. anthracis* dip	2.778	2.950
Heated *B. anthracis* flat	2.179	2.971
B. thuringiensis ridge	4.297	4.952
B. thuringiensis dip	3.962	4.953
B. thuringiensis flat	4.801	5.510
Heated *B. thuringiensis* ridge	3.268	3.788
Heated *B. thuringiensis* dip	3.509	3.920
Heated *B. thuringiensis* flat	3.384	3.700

V. Discussion

Overview

Although the data presented in this paper was limited due to the small number of spores examined, the results indicate that *B. anthracis* and *B. thuringiensis* spores have structural differences. They differ enough in surface elasticity to be able to distinguish the two species. The results also indicate that heating does affect the spores' surface properties. Further work should be done to better understand the spore structural differences between the two species and the effect heat has on them.

Assumptions Made in the Experimental Method

In this research all contact between the AFM tip and the spore surface was assumed to be elastic so that it could be modeled using the Hertz contact model. In reality, the behavior was visco-elastic, deforming as the surfaces came together and then returning to their original shape when they were no longer interacting. This assumption allowed a rough estimate of elasticities to be calculated, but more importantly, allowed the differences in surface properties to be compared between the two spore species.

Another assumption made in the calculations was that the reflection amplitude curves for the spore samples were the same shape as the reflection amplitude curves for the reference materials, polystyrene and graphite. Although this appeared to be true for the stiff tips, it wasn't with the softer tips where peaks appeared in the curves due to interaction with adsorbed water. Making this assumption allowed the impedances to be canceled out in the calculations.

Linking Observations to Theory

The soft tips gave lower elasticity values. This was probably due to adsorbed water on the surface of the spore. However, in some cases it may have also been due to the outermost layer of the exosporium which previous research has shown to be made up of short hair-like structures (Hachisuka, Kojima and Sato, 1966:2382). I would expect these structures to be less stiff and consequently have a smaller Young's modulus. They may also display more adhesion to the AFM tip than the underlying spore coat does.

The *B. thuringiensis* spores had a much higher elasticity than the *B. anthracis* spores. This indicates that they have a different outer spore coat structure. I suppose that the *B. anthracis* spore has a similar architecture to the *B. cereus* spore as shown by Plomp, Leighton, Wheeler, and Malkin. The outermost spore coat layer of *B cereus* is composed of parallel rodlet packets. Beneath this is a layer with rigid honeycomb structure. I would expect the rodlet layer to be softer due to its patchwork appearance and construction. *B. thuringiensis* was shown to have only the honeycomb structure in its spore coat (Plomp and others, 2005b:605). Previous research on *B. anthracis* spores using the electron microscope have shown the spore coat is composed of two layers (Giorno and others, 2007:691).

Heat appears to degrade the outer spore coat. This may, in part, contribute to spore death by weakening the ability of the coat to keep molecules from entering the spore core. Once molecules have entered the core, they can trigger the changes the spore goes through in germination. These changes cause the spore to begin lose its ability to survive in extreme conditions, and make it more vulnerable to other threats in its environment.

During heating, the entire spore would have been at the same temperature. Damage to the protein structure in the outer spore coat layer provides evidence for general damage to all unprotected protein in the spore from high temperatures. Although the spore coat is not critical to heat resistance (Driks, 1999:15), damage to proteins could effect overall survival and eventual germination of the spore.

Recommendations For Future Work

This research is a preliminary study of heat effects on spore surface properties. Data should be collected for more spores to give a better idea of the variance in elasticity between spores of a species and between those that have been heat inactivated. Further research should also be done to examine how extensive the heat damage is to the spore structure, using stiffer tips to look at deeper layers as well as a sonication probe to help remove the outermost layers of the spore.

More temperature and time conditions should be examined to better determine how changes in temperature and time exposure affect the spore surface properties. In this experiment only one temperature and time for heat inactivation was used for each of the spore species, 160^{o} C for 45 seconds for *B. anthracis* and 140^{o} C for 60 seconds for *B. thuringiensis*. Shorter times were impossible to use since the samples had been mounted on steel disks. In the future the samples will need to be prepared differently for heat inactivation, perhaps by performing heat inactivation before securing them to the steel mounting disk or by using a laser for heating.

The effect of humidity in the environment on the spore should also be determined. The more water present in the environment, the more hydrated the spore is likely to be. This should stretch the spore coat out, or at least keep it from any folding.

Comparisons should also be made for spores grown in different types of media since previous research has shown that this can affect the spore structure and thickness of the spore coat (Driks, 1999:6). It would be interesting to determine the exact architecture of the *B. anthracis* spore by using a sonicator probe to first remove the exosporium and then the outer layer of the spore coat and imaging the spore with the AFM following a method similar to that used by Plomp, Wheeler, Leighton, and Malkin. This would help confirm whether I am correct in assuming that structurally *B. anthracis* spores are more similar to *B. cereus* spores than *B. thuringiensis* spores. Along with this, *B. cereus* spores should also be measured for surface elasticity to compare with *B. thuringiensis* and *B. anthracis*.

Conclusions

Although *B. anthracis* and *B. thuringiensis* differ in surface properties, *B. thuringiensis* is still a good choice to use as a simulant. Further research may confirm the surface properties of *B. anthracis* are more similar to those of *B. cereus* than *B. thuringiensis*. However, *B. thuringiensis* is harmless to humans while *B. cereus* can cause food poisoning and skin infections. Due to safety considerations, *B. thuringiensis* is the better choice. This research should help those using *B. thuringiensis* as a simulant to better understand its limits and differences from the species it is being used to model by giving a better understanding of those differences.

All three objectives of this research were met. I was able to determine that *B. anthracis* and *B. thuringiensis* spores differ in surface elasticity. This difference is enough that I think it could be used to distinguish between the two species. I had expected to see some differences in elasticity over the spore surface, but my results

showed that the spore surface properties are relatively uniform. As I've gained a better understanding of spore structure this makes sense, since unlike with a cell that would have receptor proteins, ion channels, and other structures on its surface, in a spore these structures are all in the interior imbedded in the inner membrane. I was also able to determine that heating does change the elastic properties of the spore surface.

Appendix A: Suppliers

To aid in further work on this research topic I have made a list of supplies that will probably need to purchased to produce more samples, their prices, and the contact information for the companies that produce them, along with comments of which products I found to work best.

Veeco Probes
store.veeco.com
Office hours M-F 8:30AM-5:30PM, PST

Customer Support/Technical Information:
Email probes@veeco.com
Phone (805) 38-VEECO / (805) 388-3326
Fax(805) 484-2089

Sales Information:
Pay by Credit Card call: (805) 38-VEECO / (805) 388-3326; (800) 715-8440
Purchase Order by fax: (805) 484-2089; (888) 221-2219

Veeco Nanofabrication Center
Veeco Probes
3601 Calle Tecate
Suite C
Camarillo, CA 93012

Description	Part Name/No.	Price	Comments
Si Nitride contact mode probe tip – package of 100	NP-1	$1550.00	
Graphite substrate	HOPG (12 mm x 12mm)	$100	Too big- better to go with HOPG from SPI
Sample Adhesive Pads - package of 50	STKYDOT	$125.00	
SPM Sample Mounting Disks, 15 mm diameter, steel, package of 50	SD-102	$100.00	Easiest to use size

Nanoscience Instruments, Inc.
store.nanoscience.com
email: sales@nanoscience.com

phone: 888-777-5573 (toll free in US & Canada)
480-940-3940

fax: 480-940-3941

Mailing Address:
Nanoscience Instruments, Inc.
9831 South 51st Street, Suite C119
Phoenix, AZ 85044
USA

Description	Part Name/No.	Price	Comments
VistaProbes T300 Tapping mode AFM probes – package of 25	T300-25	$460.00	
Steel Mounting Discs, 10 mm diam. – package of 100	NS00594	$80.00	Too small, difficult to use. Better to order from Veeco

……

SPI Supplies
http://www.2spi.com
email: spi3spi@2spi.com
phone: 1-(800)-2424-SPI
1-(610)-436-5400

fax: 1-(610)-436-5755

Mailing Address:
SPI Supplies
P.O. Box 656,
West Chester, PA 19381-0656

Description	Part Name/No.	Price	Comments
HOPG – ZYH Grade SPI-3, 10x10x2 mm	440HP-AB	$135.66	Easiest to work with and cleave

Appendix B: Elasticity Calculation

The reflection and transmission coefficients for an imperfect interface, which is one that has finite interfacial stiffness, is given by the following two equations (Li and Burggraf, 2007:4).

$$R_{12} = \frac{Z_2 - Z_1 + i(\omega / K_n) Z_1 Z_2}{Z_2 + Z_1 - i(\omega / K_n) Z_1 Z_2}$$

$$T_{12} = \frac{2Z_2}{Z_2 + Z_1 - i(\omega / K_n) Z_1 Z_2}$$

Where R_{12} is the reflection coefficient, T_{12} is the transmission coefficient, Z_1 and Z_2 are impedances, ω is frequency,and K_n is the stiffness of the interface.

Assuming the impedances Z_1 and Z_2 are about equal, as is the case if the reflection amplitude curves are the same shape:

$$R_{12} = \frac{0 + (\omega / K_n) Z^2}{2 - i(\omega / K_n) Z^2} = \frac{(\omega / K_n) Z^2}{2 - i(\omega / K_n) Z^2}$$

The slope of the reflectance as $\omega \to 0$: $\frac{\partial R}{\partial \omega} = \frac{i}{2} \frac{Z^2}{K_n}$

So $K_n \alpha (\text{slope})^{-1}$

Stiffness can be determined by $K_n = 2rE^* = \alpha\sqrt[3]{6FRE^{*2}}$ from the Hertz contact model, where r is contact radius, $\alpha = \sqrt{A_r / A_a}$ which is a factor correction between the difference of real and apparent areas of contact, R is the radius of the AFM tip, F is the normal force, and E* is the reduced Young's modulus given by $1/E^*=1/M_t+1/M_s$ where M_t and M_s are the indentation modulus of the tip and substrate respectively (Li and Burggraf, 2007:5).

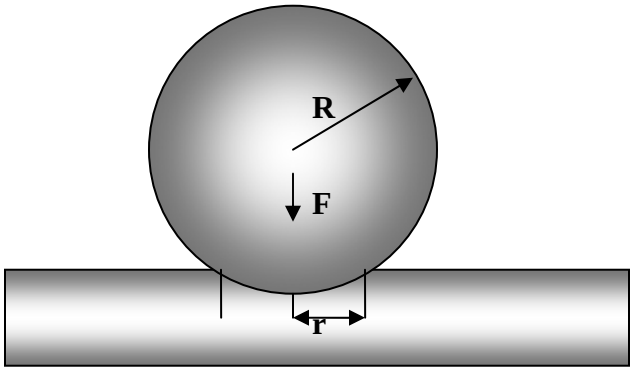

Figure 20. Hertz Contact Model.

However, it is difficult to know the exact tip geometry, so a comparison between a reference sample for which elasticity is known and the unknown sample is made.

$$E_s^* = E^*_{ref}\left(\frac{\alpha_{ref}K_s}{\alpha_s K_{ref}}\right)^n$$

Where n is determined by tip geometry and α by contact geometry (Li and Burggraf, 2007:6).

Estimating the contact area ratio (α_{ref}/α_s) to be close to 1 and using n=1.5 for a parabolic tip gives:

$$E_s^* = E^*_{ref} \left(\frac{K_s}{K_{ref}}\right)^{1.5}$$

The value used for E^*_{ref} was 3 GPa, which was the average value of Young's modulus for polystyrene determined by Dr. Li (Li and Burggraf, 2007:8).

Appendix C: Spore Elasticity Data

Below are AFM height images of all the spores that were measured in this research, along with a table of the elasticity values calculated for the measurements. Measurements were typically taken at four or five points on the spore surface with different height features. At each of these points on the spore surface, data was recorded three times as the input frequency dropped from 1000 Hz to 1 Hz. All elasticity values are given in GPa (10^9 Pascals). The table rows have been shaded to make it clear which measurements were taken at the same point on the surface of the spores.

B. anthracis

Table 6. Elasticity values for *B. anthracis* spore 1 taken with soft tip.

Elasticity	Average	Surface Feature
2.660694 2.40876 2.528821	2.532758	ridge
2.531688 2.354177 2.427187	2.437684	dip
2.102415 2.593122 2.819159	2.504899	ridge
2.888708 2.700033 2.901242	2.829994	dip
2.700033 2.643949 2.992587	2.778856	

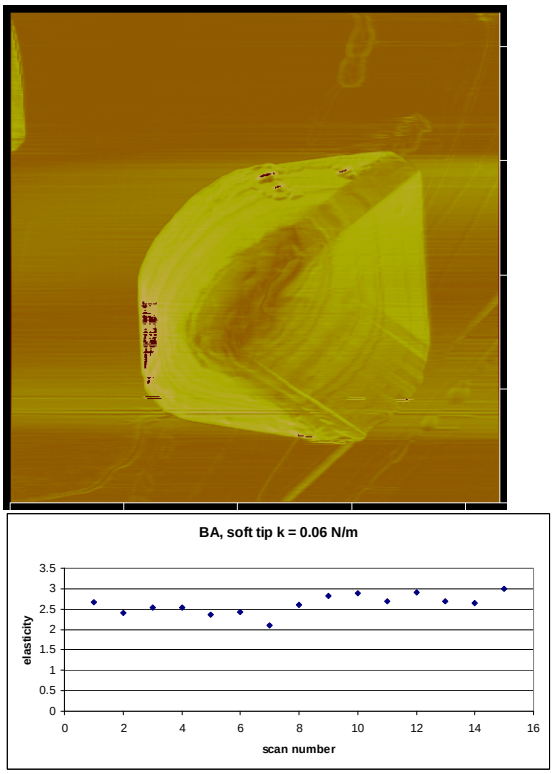

Figure 21. *B. anthracis* spore 1 AFM image and elasticity graph.

Table 7. Elasticity values for *B. anthracis* spore 2 taken with soft tip.

Elasticity	Average	Surface Feature
3.044801		
3.166139	3.147212	ridge
3.230696		
0.804998		
0.730888	0.765707	slight ridge
0.761234		
0.862954		
0.838961	0.780773	dip
0.640404		
0.660257		
0.673845	0.695514	dip
0.752439		

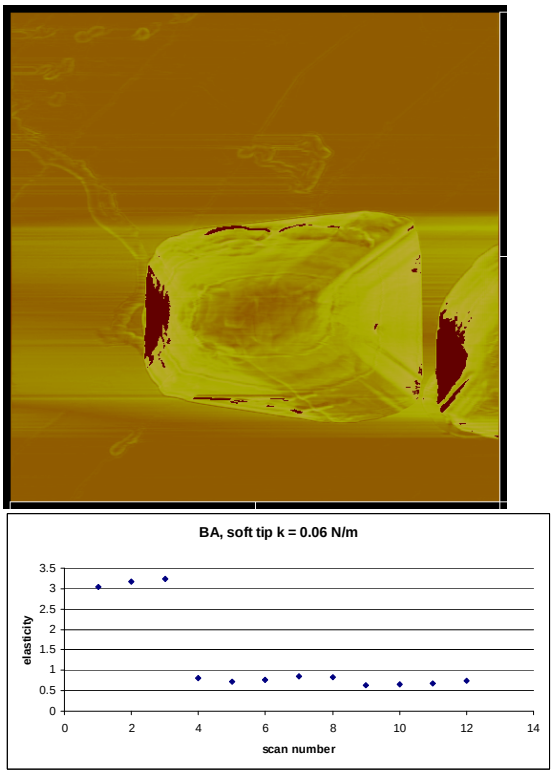

Figure 22. *B. anthracis* spore 2 AFM image and elasticity graph.

Table 8. Elasticity values for *B. anthracis* spore 3 taken with stiff tip.

Elasticity	Average	Surface Feature
3.965742		
4.067481	3.839584	ridge
3.485528		
3.75892		
3.513971	3.586164	ridge
3.485601		
3.851878		
3.814261	3.862849	dip
3.922409		
3.60192		
3.709258	3.607673	dip
3.683364		
3.43615		

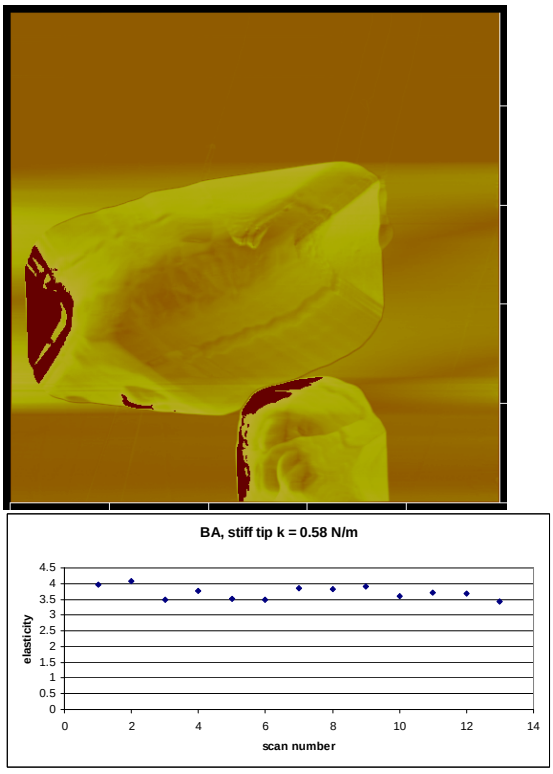

Figure 23. *B. anthracis* spore 3 AFM image and elasticity graph.

Table 9. Elasticity values for *B. anthracis* spore 4 taken with stiff tip.

Elasticity	Average	Surface Feature
3.787769		
3.717969	3.733315	ridge
3.694207		
3.870579		
3.717969	3.704448	dip
3.524797		
4.313315		
3.577496	3.784793	flat
3.463569		

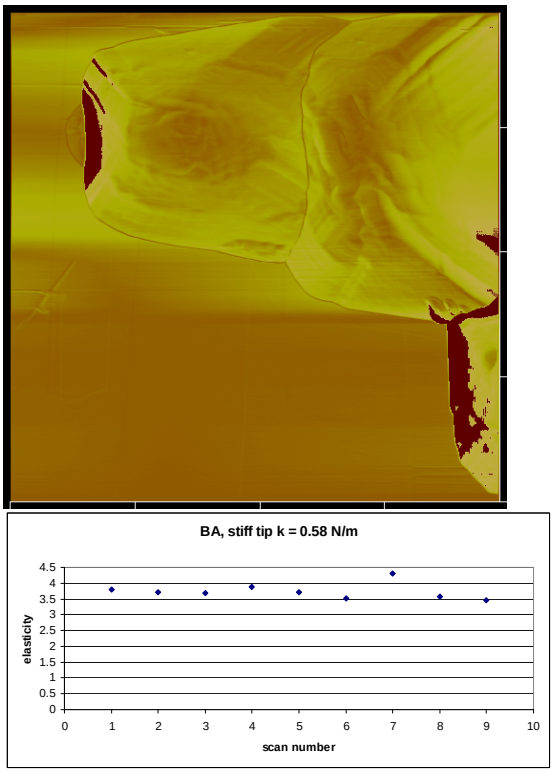

Figure 24. *B. anthracis* spore 4 AFM image and elasticity graph.

Heat inactivated *B. anthracis*

Table 10. Elasticity values for heat inactivated *B. anthracis* spore 1 taken with soft tip.

Elasticity	Average	Surface Feature
1.61663 1.465136 1.466838	1.516202	ridge slope
1.340584 1.35516 1.597038	1.430927	ridge
1.362233 1.182144 1.155414	1.233264	dip
1.45752 1.363943 1.301654	1.374372	ridge
1.033466 1.048781 0.837689	0.973312	dip

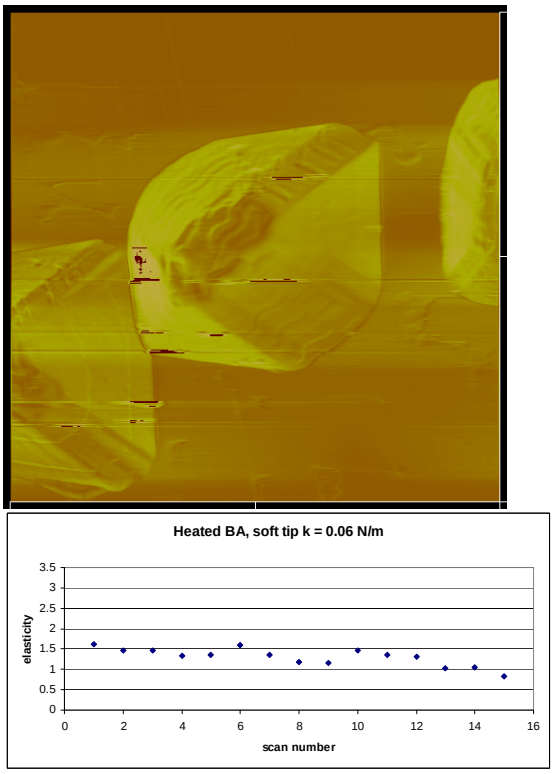

Figure 25. Heated *B. anthracis* spore 1 AFM image and elasticity graph.

Table 11. Elasticity values for heat inactivated *B. anthracis* spore 2 taken with stiff tip.

Elasticity	Average	Surface Feature
2.145132 2.170299 2.076383	2.130605	ridge
2.111855 2.263674 3.191065	2.522198	flat
3.037522 3.154024 2.979281	3.056942	dip
2.028931 1.916658 2.94298	2.296189	ridge
2.902934 3.203581 3.113169	3.073228	shallow dip

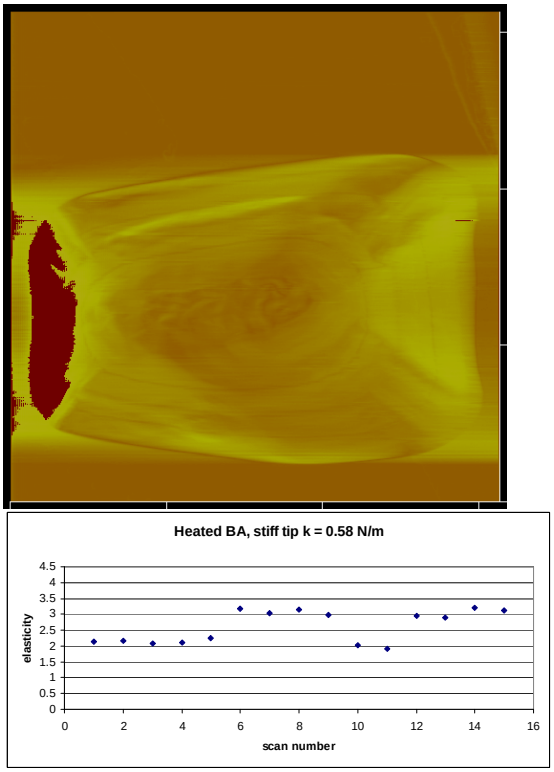

Figure 26. Heated *B. anthracis* spore 2 AFM image and elasticity graph.

Table 12. Elasticity values for heat inactivated *B. anthracis* spore 3 taken with stiff tip.

Elasticity	Average	Surface Feature
2.653619 2.640167 2.653619	2.649135	ridge
2.762201 2.604452 2.791457	2.71937	ridge
2.603406 2.523117 2.735441	2.620654	dip
3.054979 2.732511 2.833084	2.873525	ridge
2.732655 2.799899 2.56533 2.636995	2.68372	ridge

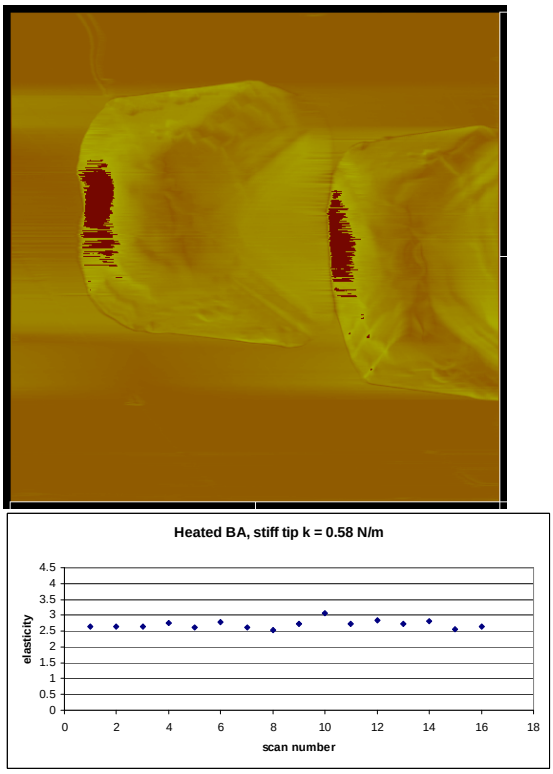

Figure 27. Heated *B. anthracis* spore 3 AFM image and elasticity graph.

Table 13. Elasticity values for heat inactivated *B. anthracis* spore 4 taken with stiff tip.

Elasticity	Average	Surface Feature
2.690246 2.543967 2.66347	2.632561	dip
2.936368 2.954184 2.894585	2.928379	edge of dip
2.70071 2.758281 2.703931	2.720974	shallow ridge
2.708711 2.55568 2.6198	2.628064	flat

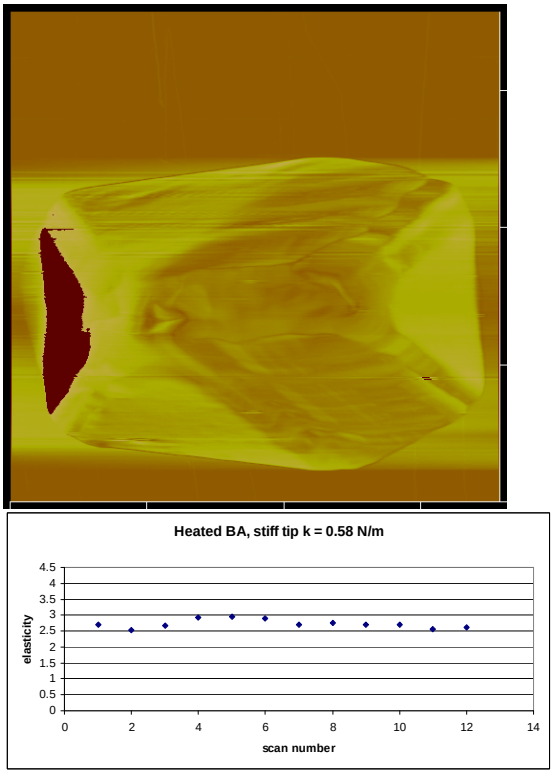

Figure 28. Heated *B. anthracis* spore 4 AFM image and elasticity graph.

Table 14. Elasticity values for heat inactivated *B. anthracis* spore 5 taken with stiff tip.

Elasticity	Average	Surface Feature
2.91277 2.830018 2.965689	2.902825	ridge
2.984063 2.78824 2.825692	2.865998	dip
2.965346 3.004202 2.745082	2.904877	ridge
2.906609 2.879754 2.827695	2.871353	dip

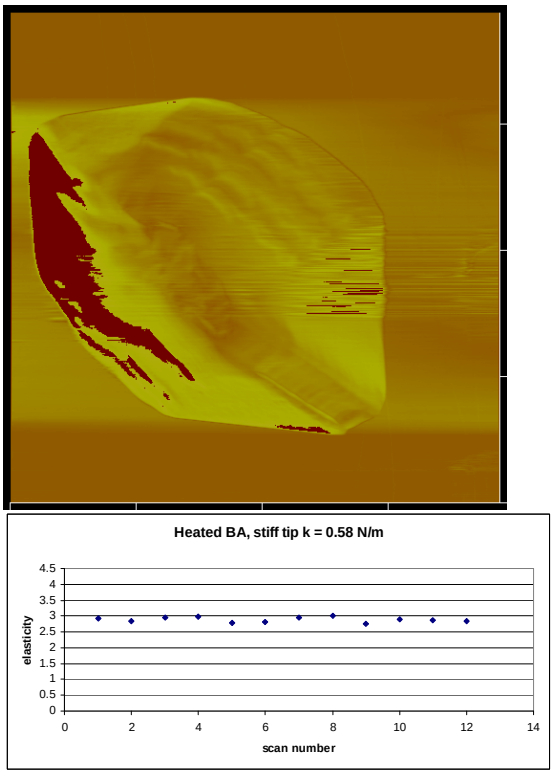

Figure 29. Heated *B. anthracis* spore 5 AFM image and elasticity graph.

B. thuringiensis

Table 15. Elasticity values for *B. thuringiensis* spore 1 taken with soft tip.

Elasticity	Average	Surface Feature
0.803957 0.763508 0.696426	0.75463	ridge
0.862832 0.881208 0.790797 0.797835 0.784576	0.82345	dip
2.088568 1.838781 1.871161	1.932837	edge
0.737951 0.707076 0.665952	0.70366	ridge
1.144204 1.012872 1.063506	1.073527	ridge

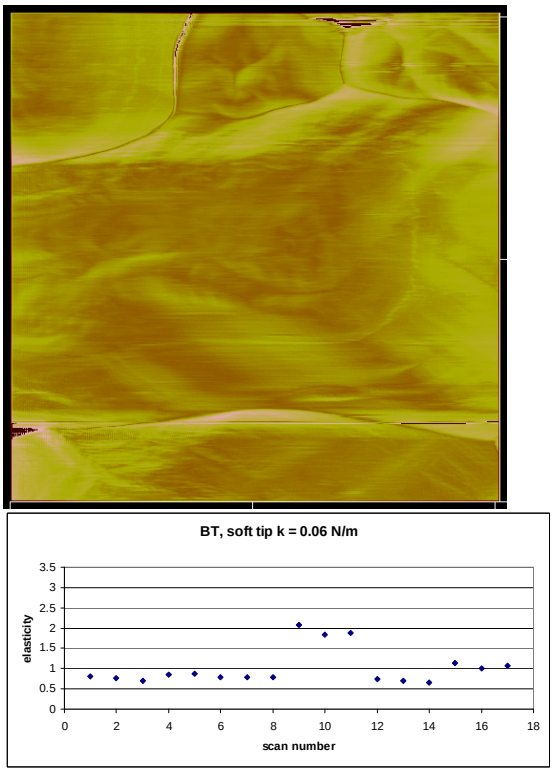

Figure 30. *B. thuringiensis* spore 1 AFM image and elasticity graph.

Table 16. Elasticity values for *B. thuringiensis* spore 2 taken with soft tip.

Elasticity	Average	Surface Feature
1.365497 1.178328 1.286292	1.276705	ridge
1.278463 1.297097 1.424862	1.333474	Dip
1.251677 1.357632 1.321659 1.361293	1.323065	Ridge
1.087723 1.1001 1.093064	1.093629	slight dip

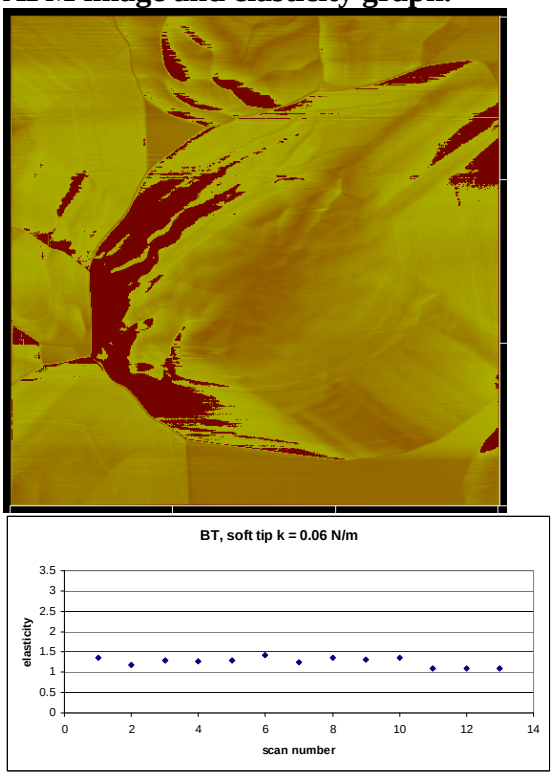

Figure 31. *B. thuringiensis* spore 2 AFM image and elasticity graph.

Table 17. Elasticity values for *B. thuringiensis* spore 3 taken with stiff tip.

Elasticity	Average	Surface Feature
3.866477		
4.009473	3.968431	dip
4.029344		
3.880056		
3.856806	3.843698	ridge
3.794231		
3.762518		
3.737922	3.70894	dip
3.626379		
3.913712		
3.785944	3.876268	ridge
3.929149		

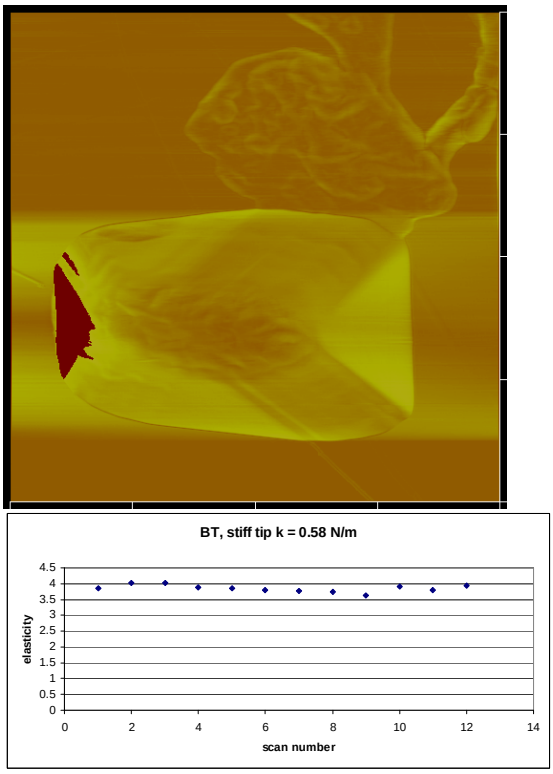

Figure 32. *B. thuringiensis* spore 3 AFM image and elasticity graph.

Table 18. Elasticity values for *B. thuringiensis* spore 4 taken with stiff tip.

Elasticity	Average	Surface Feature
4.007271		
4.314377	4.084242	ridge
3.931079		
4.154866		
5.280002	4.624533	dip
4.438731		
5.400773		
5.445028	5.159035	ridge
5.210173		
4.580165		
4.331921		
4.262437	4.305958	ridge
4.323516		
5.391033		
5.452448	5.334848	flat
5.161063		

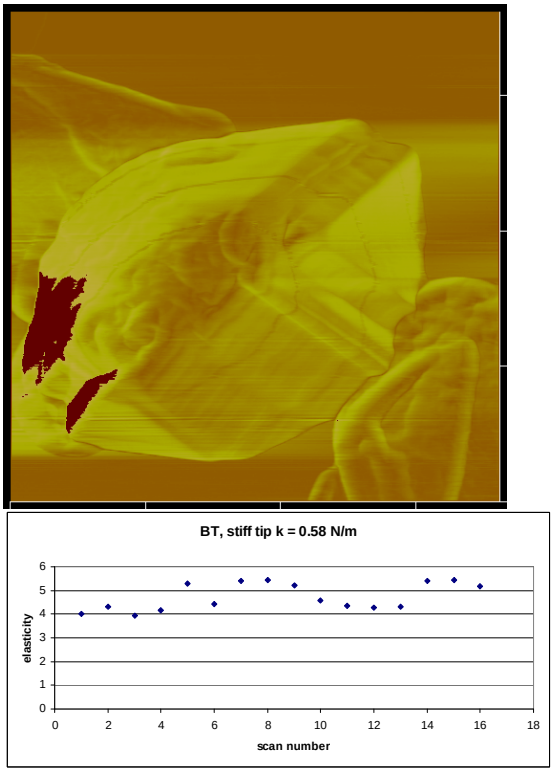

Figure 33. *B. thuringiensis* spore 4 AFM image and elasticity graph.

Table 19. Elasticity values for *B. thuringiensis* spore 5 taken with stiff tip.

Elasticity	Average	Surface Feature
5.32343		
5.266309	5.414621	ridge
5.654122		
5.205744		
5.364821	5.253311	flat
5.189367		
5.792909		
5.296975	5.410915	ridge
5.142862		
5.714905		
5.469349	5.52851	dip
5.401276		

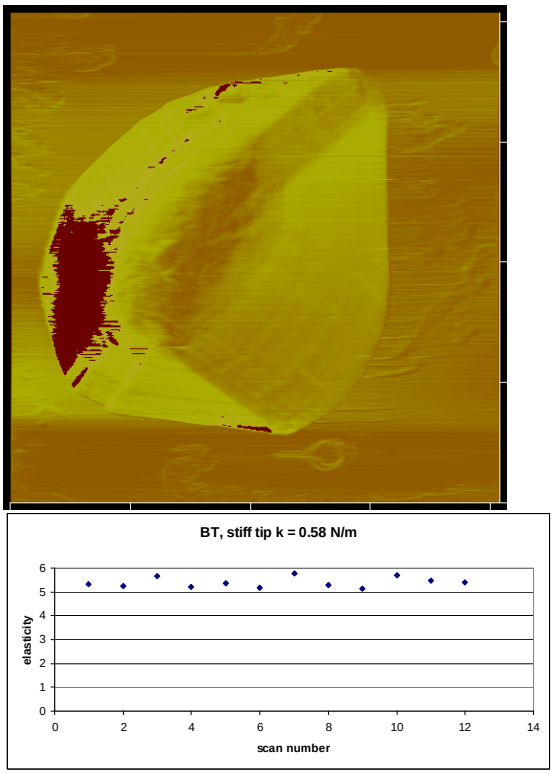

Figure 34. *B. thuringiensis* spore 5 AFM image and elasticity graph.

Heat inactivated *B. thuringiensis*

Table 20. Elasticity values for heat inactivated *B. thuringiensis* spore 1 taken with soft tip.

Elasticity	Average	Surface Feature
2.404774		
2.395902	2.496863	
2.689912		
10.49942		
10.20404	10.33368	dip
10.29758		
2.176827		
2.714875	2.476261	ridge
2.53708		
0.090122		
0.111757		
0.116544	0.123244	
0.174554		
3.74879		
4.365383	4.477568	
5.318531		

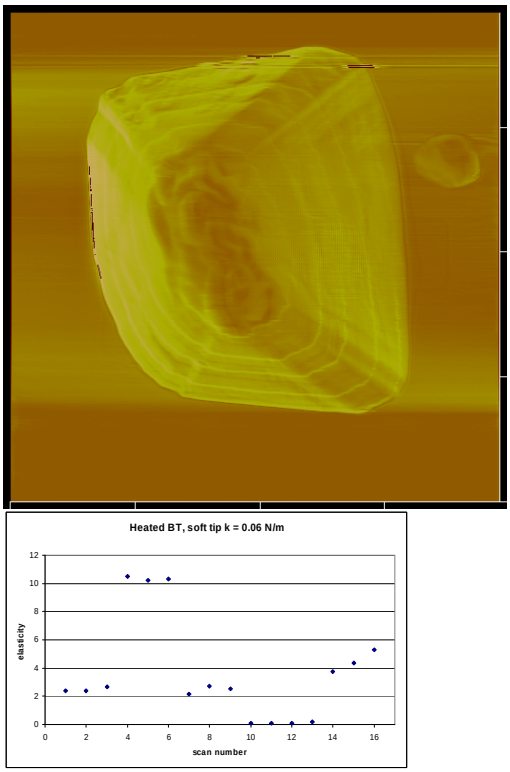

Figure 35. Heated *B. thuringiensis* spore 1 AFM image and elasticity graph.

Table 21. Elasticity values for heat inactivated *B. thuringiensis* spore 2 taken with stiff tip.

Elasticity	Average	Surface Feature
3.408779		
3.460638	3.38169	ridge
3.275654		
3.610571		
3.485184	3.542084	flat
3.530497		
3.804784		
3.696815	3.714532	dip
3.641996		
3.727622		
3.580392	3.869016	ridge
4.299034		
3.101224		
3.414692	3.332482	ridge
3.481528		

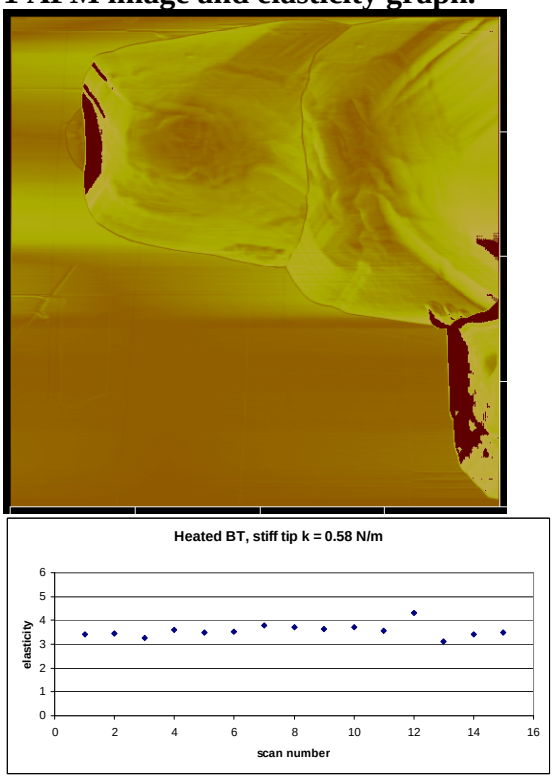

Figure 36. Heated *B. thuringiensis* spore 2 AFM image and elasticity graph

Bibliography

"2001 anthrax attacks." *Wikipedia*. n. pag. http://en.wikipedia.org/wiki/2001_anthrax_attacks. 20 August 2007.

Abu-Lail, Nehal I., and Terri A. Camesano. "Elasticity of *Pseudomonas putida* KT2442 Surface Polymers with Single-Molecule Force Microscopy." *Langmuir.* 18:4071-4081 (2002).

A-Hassan, Emad, William F. Heinz, Matthew D. Antonik, Neill P. D'Costa, Soni Nageswaran, Cora-Ann Schoenberger, and Jan H. Hoh. "Relative Microelastic Mapping of Living Cells by Atomic Force Microscopy." *Biophysical Journal*. 74: 1564-1578 (Mar. 1998).

Amro, Nabil A., Lakshmi P. Kotra, Kapila Wadu-Methridge, Alexy Bulychev, Shahriar Mobashery, and Gang-yu Liu. "High-Resolution Atomic Force Microscopy Studies of the *Escherichia coli* Outer Membrane: Structural Basis for Permeability." *Langmuir.* 16:2789-2796 (2000).

"Appendix 1 – Media." *Molecular Biological Methods for Bacillus.* Ed. C. R. Harwood and S. M. Cutting. John Wiley & Sons, 1990.

Arnoldi, Markus, Monika Fritz, Edmund Bäuerlain, Manfred Radmacher, Erich Sackman, and Alexei Boulbitch. "Bacterial turgor pressure can be measured by atomic force microscopy." *Physical Review E.* 62:1034-1044 (Jul. 2000).

Binnig, G., and C. F. Quate. "Atomic Force Microscope." *Physical Review Letters.* 56:930-933 (Mar. 1986).

Buck, C. A., R. L. Anacker, F. S. Newman, and A. Eisenstark. "Phage Isolated From Lysogenic *Bacillus anthracis*." *Journal of Bacteriology.* 85:1423-1430 (1963).

Camesano, Terri A., Michael J. Natan, and Bruce E. Logan. "Observation of Changes in Bacterial Cell Morphology Using Tapping Mode Atomic Force Microscopy." *Langmuir.* 16:4563-4572 (2000).

Castanha, Elisanga R., Marvin Vestal, Steve Hattan, Alvin Fox, Karen F. Fox, and Danielle Dickinson. "*Bacillus cereus* strains fall into two clusters (one closely and one more distantly related) to *Bacillus anthracis* according to amino acid substitutions in small acid-soluble proteins as determined by tandem mass spectrometry." *Molecular and Cellular Probes.* 21:190-201 (2007).

Chada, Venkata G. R., Erik A. Sanstad, Rong Wang, and Adam Driks. "Morphogenesis of *Bacillus* Spore Surfaces." *Journal of Bacteriology.* 185:6255-6261 (Nov. 2003).

Claus, Dieter and Dagmar Fritze. "Taxonomy of *Bacillus.*" *Bacillus.* Ed. Colin R. Harwood. New York: Plenum Press, 1989.

Cleveland, J. P., S. Manne, D. Bocek, and P. K. Hansma. "A nondestructive method for determing the spring constant of cantilevers for scanning force microscopy." *Review of Scientific Instruments.* 64:403-405 (Feb. 1993).

Davison, Sophie, Evelyne Couture-Tosi, Thomas Candela, Michèle Mock, and Agnès Fouet. "Identification of the *Bacillus anthracis* γ Phage Receptor." *Journal of Bacteriology.* 187:6742-6749 (Oct. 2005).

Doi, Roy H. "Sporulation and Germination." *Bacillus.* Ed. Colin R. Harwood. New York: Plenum Press, 1989.

Driks, Adam. "The *Bacillus* Spore Coat." *Phytopathology.* 94:1249-1251 (2004).

----. "*Bacillus subtilis* Spore Coat." *Microbiology and Molecular Biology Reviews.* 63:1-20 (Mar. 1999).

----. "Maximum shields: the assembly and function of the bacterial spore coat." *Trends in Microbiology*. 10:251-254 (Jun. 2002).

Dufrêne, Yves F. "Application of atomic force microscopy to microbial surfaces: from reconstituted cell surface layers to living cells." *Micron.* 32:153-165 (2001).

----. "Atomic Force Microscopy." *Methods for General and Molecular Microbiology* (3rd Edition). Ed. C. A. Reddy, T. A. Beveridge, J. A. Breznak, G. A. Marzluf, and T. M. Schmidt. ASM Press, 2007.

----. "Atomic Force Microscopy, a Powerful Tool in Microbiology." *Journal of Bacteriology.* 184:5205-5213 (Oct. 2002).

Dufrêne, Yves F., Christophe J. P. Boonaert, Patrick A. Gerin, Marcel Asther, and Paul G. Rouxhet. "Direct Probing of the Surface Ultrastructure and Mlecular Interaction of Dormant and Germinating Spores of *Phanerochaete chrysosporium.*" *Journal of Bacteriology.* 181:5350-5354 (Sept. 1999).

Dwyer, Kathleen G., Janine M. Lamonica, Jennifer A. Shumacher, Leanne E. Williams, Joanne Bishara, Anna Lewandowski, Rajendra Redkar, Guy Patra, and Vito G. DelVecchio. "Identification of *Bacillus anthracis* specific chromosomal sequences by suppressive subtractive hybridization." *BMC Genomics*. 5:15-26 (2004).

Eid, Hassan and Andy Pamp. "An Introductory Overview of Contact Mechanics and Adhesion." Mechanics of Contact and Lubrication, MGM G230. Department of Mechanical and Industrial Engineering. Northeastern University. Spring 2006.

Fasolka, Michael J., Anne M. Mayes, and Sergei N. Maganov. "Thermal enhancement of AFM contrast for imaging diblock copolymer thin film morphology." *Ultramicroscopy.* 90:21-31 (2001).

Ferrari, Eugenio and James A. Hoch. "Genetics." *Bacillus.* Ed. Colin R. Harwood. New York: Plenum Press, 1989.

Firtel, M., and T. J. Beveridge. "Scanning Probe Microscopy in Microbiology." *Micron.* 26:347-362 (1995).

Gerhardt, Phillip and Edgar Ribi. "Ultrastructure of the Exosporium Enveloping Spores of *Bacillus cereus*." *Journal of Bacteriology.* 88:1774-1789 (Dec. 1964).

Giorno, Rebecca, Joel Bozue, Christopher Cote, Theresa Wenzel, Krishna-Sulayman Moddy, Michael Mallozzi, Matthew ryan, Rong Wang, Ryszard Zielke, Janine R. Maddock, Arthur Friedlander, Susan Welkos, and Adam Driks. "Morphogenesis of the *Bacillus anthracis* Spore." *Journal of Bacteriology.* 189:691-705 (Feb. 2007).

Greenspan, Lewis. "Humidity Fixed Points of Binary Saturated Aqueous Solutions." *Journal of Research of the National Bureau of Standards – A. Physics and Chemistry*. 81A:89-96 (1976).

Hachisuka, Yoetsu, Kiyohide Kojima, and Taizan Sato. "Fine Filaments on the Outside of the Exosporium of *Bacillus anthracis* Spores." *Journal of Bacteriology.* 91:2382-2384 (June 1966).

Harwood, Colin R., A. Ronald Archibald, Ian C. Hancock, and Daniel R. Zeigler. "Growth, Maintenance and General Techniques." *Molecular Biological Methods for Bacillus.* Ed. C. R. Harwood and S. M. Cutting. John Wiley & Sons, 1990.

Hawkins, Leslie S. *Micro-etched platforms for thermal inactivation of Bacillus anthracis and Bacillus thuringiensis spores.* MS Thesis, AFIT/GWN/ENP/08-M01. School of Engineering and Management, Air Force Institute of Technology (AU), Wright-Patterson AFB, OH, March 2008.

Henriques, Adriano O. and Charles P. Moran, Jr. "Structure and Assembly of the Bacterial Endospore Coat." *Methods.* 20:95-110 (2000).

Hodges, L. R., L. J. Rose, A. Peterson, J. Noble-Wang, and M. J. Arduino. "Evaluation of a Macrofoam swab Protocol for the Recovery of *Bacillus anthracis* Spores form a Steel Surface." *Applied and Environmental Microbiology.* 72:4429-4430 (June 2006).

Kester, E., U. Rabe, L. Presamanes, Ph. Tailhades, and W. Arnold. "Measurement of Mechanical Properties of Nanocscaled Ferrites using Atomic Force Microscopy at Ultrasonic Frequencies." *NanoStructured Materials.* 12:779-782 (1999).

Kim, Kijeong, Juwon Seo, Katherine Wheeler, Chulmin Park, Daewhan Kim, Seungjoon Park, Wonyong Kim, Sang-In Chung, and Terrance Leighton. "Rapid genotypic detection of *Bacillus anthracis* and the *Bacillus cereus* group by multiplex real-time PCR melting curve analysis." *FEMS Immunology and Medical Microbiology.* 43:301- 310 (Feb 2005).

Koehler, Theresa M. "*Bacillus anthracis.*" *Gram-Positive Pathogens.* Ed. Vincent A Fischetti, Richard P. Novick, Joseph J Ferretti, Daniel A. Portnoy, and Julian I. Rood. Wachington, D.C.: ASM Press, 2000.

Kutima, Philip M. and Peggy M. Foegeding. "Involvement of the Spore Coat in Germination of *Bacillus cereus* T Spores." *Applied and Environmental Microbiology.* 53:47-52 (Jan. 1987).

Kuznetsova, Tatyana G., Maria n. Starodubtseva, Nicolai I. Yegorenkov, Sergey A. Chizhik, and Renat I. Zhdanov. "Atomic force microscopy probing of cell elasticity." *Micron.* Article in press. (2007).

Lai, Erh-Min, Nikhil D. Phadke, Maureen T. Kachman, Rebecca Giorno, Santiago Vazquez, Jenny A. Vazquez, Janine R. Maddock, and Adam Driks. "Proteomic Analysis of the Spore Coats of *Bacillus subtilis* and *Bacillus anthracis*." *Journal of Bacteriology.* 185:1443-1454 (Feb. 2003).

Laue, Michael, Bärbel Niederwöhrmeier, and Norbert Bannert. "Rapid diagnostic thin section electron microscopy of bacterial endospores." *Journal of Microbiological Methods.* 70:45-54 (2007).

Lavrentyev, Anton I. and S. I Rokhlin. "Ultrasonic spectroscopy of imperfect contact interfaces between a layer and two solids." *Journal of the Acoustical Society of America*. 103:657-664 (1998).

Leuschner, Renata G. K. and Peter J. Lillford. "Thermal properties of bacterial spores and biopolymers." *International Journal of Food Microbiology.* 80:131-143 (2003).

Li, Guangming, and Larry W. Burggraf. "Controlled pattering of polymer films using an AFM tip as a nano-hammer." *Nanotechnology.* (June 2007).

----. "Nanometer-Scale Elastic Modulus of Surfaces and Thin Films determined using an Atomic Force Microscope." in review, *Thin Film Science*. (2007).

Liu, Hongbin, Nicholas H. Bergman, Brendan Thomason, Shamira Shallom, Alyson Hazen, Joseph Crossno, David A. Rasko, Jacques Ravel, Timothy D. Read, Scott N. Peterson, John Yates III, and Philp C. Hanna. "Formation and Composition of the *Bacillus anthracis* endospore." *Journal of Bacteriology.* 186:164-178 (Jan. 2004).

Lo, Yu-Shui, Neil D. Huefner, Winter S. Chan, Paul Dryden, Birgit Hagenhoff, and Thomas P. Beebe, Jr. "Organic and Inorganic Contamination on Commercial AFM Cantilevers." *Langmuir.* 15:6522-6526 (1999).

Magonov, Sergei N. and Myung-Hwan Whangbo. *Surface Analysis with STM and AFM.* Weinheim: VCH, 1996.

McPherson, D. C., H. Kim, M. Hahn, R. Wang, P. Grabowski, P. Eichenberger, and A. Driks. "Characterization of the *Bacillus subtilis* Spore Morphogenetic Coat Protein CotO." *Journal of Bacteriology.* 187:8278-8290 (Dec. 2005).

Miller, Julie Ann. "Microbe exhibits out-of-body activity." *Science News.* 165:142 (Feb. 2004).

Missiakas, Dominique M., and Olaf Schneewind. "*Bacillus anthracis* and the Pathogenesis of Anthrax." *Biological Weapons Defense.* Ed. Luther E. Linder, Frank J. Lebeda, and George W. Korch. Totowa, New Jersey: Humana Press, 2005.

Moberly, Betty J., F. Shafa, and Philipp Gerhardt. "Structural Details of Anthrax Spores During Stages of Transformation into Vegetative Cells." *Journal of Bacteriology.* 92:220-228 (July 1966).

Model SR850 DSP Lock-In Amplifier. Rev. 1.8. Sunnyvale, CA: Stanford Research Systems, 2007.

Moir, A. "How do spores germinate?" *Journal of Applied Microbiology.* 101:526-530 (2006).

Moir, A., B. M. Corfe, and J. Behravan. "Spore germination." *Cellular and Molecular Life Sciences.* 59:403-409 (2002).

Möller, Clemens, Mike Allen, Virgil Eilings, Andreas Engel, and Daniel J. Müller. "Tapping-Mode Atomic Force Microscopy Produces Faithful High-Resolution Images of Protein Surfaces." *Biophysical Journal.* 77:1150-1158 (Aug. 1999).

Morris, V. J., A. R. Kirby, and A. P. Gunning. Atomic *Force Microcopy for Bioligists*. Norwich, UK: Imperial College Press, 1999.

Müller, Daniel J., Wolfgang Baumeister, and Andreas Engel. "Controlled unzipping of a bacterial surface layer with atomic force microscopy." *PNAS.* 96:13170-13174 (Nov. 1999).

Multimode Scanning Probe Microscope Instruction Manual. Version 4.31ce. Digital Instruments, 1996-1997.

Murayama, Yoshinobu, and Sadao Omata. "Fabrication of micro tactile sensor for the measurement of micro-scale local elasticity." *Sensors and Actuators A.* 109:202-207 (2004).

Nicholson, Wayne L. and Peter Setlow. "Sporulation, Germination and Outgrowth." *Molecular Biological Methods for Bacillus.* Ed. C. R. Harwood and S. M. Cutting. New York: John Wiley & Sons, 1990.

Padfield, Tim. "Saturated salt solutions for controlling relative humidity." *Conservation Physics.* http://www.padfield.org/tim/cfys/satslt/satsol.php. 17 September 2007.

Pharr, G. M., W. C. Oliver, and F. R. Brotzen. "On the generality of the relationship among contact stiffness, contact area, and elastic modulus during indentation." *Journal of Materials Research.* 7:613-617 (Mar 1992).

Plomp, Marco, Terrance J. Leighton, Katherine E. Wheeler, and Alexander J. Malkin. "Architecture and High-Resolution Structure of *Bacillus thuringiensis* and *Bacillus cereus* Spore Coat Surfaces." *Langmuir*. 21: 7892-7898 (2005a).

----. "The High-Resolution Architecture and Structural Dynamics of *Bacillus* Spores." *Biophysical Journal*. 88: 603-608 (2005b).

Plomp, Marco, Terrance J. Leighton, Katherine E. Wheeler, Haley D. Hill, and Alexander J. Malkin. "In vitro high-resolution structural dynamics of single germinating bacterial spores." *PNAS*, 104: 9644-9649 (June 2007).

Pobojewski, Sally. "Anthrax spores can germinate, grow and reproduce in soil." *The University Record Online.* University of Michigan Press Release, (16 Feb. 2004). 9 Oct 2007. http://www.umich.edu/~urecord/0304/Feb16_04/21.shtml.

Priest, Fergus G. "Isolation and Identification of Aerobic Endospore-Forming Bacteria." *Bacillus.* Ed. Colin R. Harwood. New York: Plenum Press, 1989.

Rabe, U., M. Kopycinska, S. Hirsekorn, and W. Arnold. "Evaluation of the contact resonance frequencies in atomic force microscopy as a method for the surface characterization (invited)." *Ultrasonics.* 40:49-54 (2002).

Radnedge, Lyndsay, Peter G. Agron, Kare K. Hill, Paul J. Jackson, Lawrence O. Ticknor, Paul Keim, and Gary L. Anderson. "Genome Differences That Distinguish *Bacillus anthracis* from *Bacillus cereus* and *Bacillus thuringiensis*." *Applied and Environmental Microbiology.* 69:2755-2764 (May 2003).

Rasko, David A., Michael R. Altherr, Cliff S. Han, and Jacques Ravel. "Genomics of the *Bacillus cereus* group of organisms." *FEMS Microbiology Reviews.* 29:303-329 (Apr. 2005).

Razatos, Anneta, Yea-Ling Ong, Mukul M. Sharma, and George Georgiou. "Molecular determinants of bacterial adhesion monitored by atomic force microscopy." *Proceedings of the National Academy of Science USA.* 95:11059-11064 (Sept. 1998).

Rose, Laura, Bette Jensen, Alicia Peterson, Shailen N. Banerjee, and Matthew J. Arduino. "Swab Materials and *Bacillus anthracis* Spore Recovery from Nonporous Surfaces." *Emerging Infectious Diseases.* 10:1023-1029 (June 6).

Santo, Leatice Y. and Roy H. Doi. "Ultrastructural Analysis During Germination and Outgrowth of *Bacillus subtilis* Spores." *Journal of Bacteriology.* 120:475-481 (Oct. 1974).

Schaer-Zammaretti, Prisca, and Job Ubbink. "Imaging of lactic acid baceria with AFM-elasticity and adhesion maps and their relationship to biological and structural data." *Ultramicroscopy.* 97:199-208 (2003).

Schuch, Raymond, Daniel Nelson, and Vincent A. Fischetti. "A bacteriolytic agent that detects and kills *Bacillus anthracis*." *Nature.* 418:884-889 (Aug. 2002).

Schuch, Raymond, and Vincent A. Fischetti. "Detailed Genomic Analysis of the Wβ and γ Phages Infecting *Bacillus anthracis*: Implications for Evolution of Environmental Fitness and Antibiotic Resistance." *Journal of Bacteriology*. 188: 3037-3051 (Apr. 2006).

Setlow, Peter. "Spore germination." *Current Opinion in Microbiology.* 6:550-556 (2003).

Snitka, V., A. Ulcinas, and V. Mizariene. "Characterization of materials' nanomechanical properties by force modulation and phse imaging atomic force microscopy with soft cantilevers." *Materials Characterization.* 48:147-152 (2002).

Sozhamannan, Shanmuga, Michael D. Chute, Farrell D McAfee, Derrick E. Fouts, Arya Akmal, Darrell R. Galloway, Alfred Mateczun, Leslie W. Baillie, and Timothy D. Read. "The *Bacillus anthracis* chromosome contains four conserved, excision-proficient, putative prophages." *BMC Microbiology.* Apr. 2006).

Stone, Marcia. "*B. anthracis* and Its Phage: Suprising Dynamics In Soil." *Microbe.* 1:308-309 (2006).

Thorne, Curtis B. "*Bacillus anthracis*." *Bacillus subtilis and other gram-positive bacteria: biochemistry, physiology and molecular genetics.* Ed. Abraham L. Sonenshein, James A. Hoch, and Richard Losick. Washington, D. C.: American Society for Microbiology, 1993.

Thwaites, J. J., U. C. Surana. "Mechanical Properties of *Bacillus subtilus* Cell Walls: Effects of Removing Residual Culture Medium." *Journal of Bacteriology*. 173: 197-203 (Jan. 1991).

Thwaites, J. J., U. C. Surana, and A. M. Jones. "Mechanical Properties of *Bacillus subtilus* Cell Walls: Effects of Ions and Lysozyme." *Journal of Bacteriology*. 173: 204-210 (Jan. 1991).

Tortonese, Marco and Michael Kirk. "Characterization of application specific probes for SPMs." *SPIE.* 3009:53-60 (Apr. 1997).

Touhami, Ahmed, Bernard Nysten, and Yves F. Dufrêne. "Nanoscale Mapping of the Elasticity of Microbial Cells by Atomic Force Microscopy." *Langmuir.* 19:4539-4543 (2003).

van der Mei, Henny C., Henk J. Busscher, Rolf Bos, Joop de Vries, Christophe J. P. Boonaert, and Yves F. Dufrêne. "Direct Probing by Atomic Force Microscopy of the Cell Surface Softness of a Fibrillated and Nonfibrillated Oral Streptococcal Strain." *Biophysical Journal.* 78:2668-2674 (May 2000).

Vinckier, Anja, and Giorgio Semenza. "Measuring elasticity of biological materials by atomic force microscopy." *FEBS Letters*. 430: 12-16 (1998).

Weisenhorn, Albrecht L., Mitra Khorsandi, Sandor Kasa, Vassilis Gotzos, and Hans-Jürgen Butt. "Deformation ans height anomaly of soft surfaces studied with an AFM." *Nanotechnology.* 4:106-113 (1993).

Wilson, David L., Kenneth S. Kump, Steven J. Eppell, and Roger E. Marchant. "Morphological Restoration of Atomic Force Microscopy Images." *Langmuir.* 11:265-272 (1995).

Wuytack, Elke Y. and Chris W. Michaels. "A study on the effects of high pressure and heat on *Bacillus subtilis* spores at low pH." *International Journal of Food Microbiology.* 64:333-341 (2001).

Yao, X., M. Jericho, D. Pink, and T. Beveridge. "Thickness and Elasticity of Gram-Negative Murein Sacculi Measured by Atomic Force Microscopy." *Journal of Bacteriology.* 181:6865-6875 (Nov. 1999).

Zaman, Mohd. Saif, Anita Goyal, Gyanendra Prakash Dubey, Pradeep K. Gupta, Harish Chandra, Taposh K. Das, Munia Ganguli, and Yogendra Singh. "Imaging and Analysis of *Bacillus anthracis* Spore Germination." *Microscopy Research and Technique*. 66:307-311 (2005).

Zhao, Liming, David Schaefer, and Mark R. Marten. "Assessment of Elasticity and Topography of *Aspergillus nidulans* Spores via Atomic Force Microscopy." *Applied and Environmental Microbiology*. 71: 955-960 (Feb. 2005).

Zolock, Ruth A. *Characterization of the surface morphology of Bacillus spores by Atomic Force Microscopy*. MS Thesis, AFIT/GEE/ENV/02M-17. School of Engineering and Management, Air Force Institute of Technology (AU), Wright-Patterson AFB OH, March 2002.

Zolock, Ruth A., Guanming Li, Charles Bleckmann, Larry Burggraf, and Douglas C. Fuller. "Atomic force microscopy of Bacillus spore surface morphology." *Micron*. 37:363-369 (2006).

REPORT DOCUMENTATION PAGE

Form Approved
OMB No. 0704-0188

The public reporting burden for this collection of information is estimated to average 1 hour per response, including the time for reviewing instructions, searching existing data sources, gathering and maintaining the data needed, and completing and reviewing the collection of information. Send comments regarding this burden estimate or any other aspect of this collection of information, including suggestions for reducing the burden, to the Department of Defense, Executive Services and Communications Directorate (0704-0188). Respondents should be aware that notwithstanding any other provision of law, no person shall be subject to any penalty for failing to comply with a collection of information if it does not display a currently valid OMB control number.

PLEASE DO NOT RETURN YOUR FORM TO THE ABOVE ORGANIZATION.

1. REPORT DATE *(DD-MM-YYYY)*	2. REPORT TYPE	3. DATES COVERED *(From - To)*
27-03-2008	Master's Thesis	Jun 2007 - Mar 2008

4. TITLE AND SUBTITLE

NANO-MECHANICAL PROPERTIES OF HEAT INACTIVATED BACILLUS ANTHRACIS AND BACILLUS THURINGIENSIS SPORES

5a. CONTRACT NUMBER

F2KTAS8016G003

5b. GRANT NUMBER

5c. PROGRAM ELEMENT NUMBER

6. AUTHOR(S)

Poindexter, Jessica L., 2nd Lieutenant, USAF

5d. PROJECT NUMBER

2006-172

5e. TASK NUMBER

5f. WORK UNIT NUMBER

7. PERFORMING ORGANIZATION NAME(S) AND ADDRESS(ES)

Air Force Institute of Technology
Graduate School of Engineering and Management (AFIT/EN)
2950 Hobson Way

8. PERFORMING ORGANIZATION REPORT NUMBER

AFIT/GAP/ENP/08-M07

9. SPONSORING/MONITORING AGENCY NAME(S) AND ADDRESS(ES)

Angelica I. Rubio
CB Senior Scientist
709th ARSS
Kirtland AFB, NM
(505)853-1042 DSN: 263-1042

10. SPONSOR/MONITOR'S ACRONYM(S)

11. SPONSOR/MONITOR'S REPORT NUMBER(S)

12. DISTRIBUTION/AVAILABILITY STATEMENT

APPROVED FOR PUBLIC RELEASE; DISTRIBUTION UNLIMITED

13. SUPPLEMENTARY NOTES

14. ABSTRACT

B. thuringiensis spores must have similar properties to B. anthracis spores to be a good simulant in counter-proliferation studies. In particular, they must behave in a similar way when exposed to high temperatures for short periods of time as would be caused by an explosion. This research project compares surface elasticities for four different spore sample types, B. anthracis spores, heat inactivated B. anthracis spores, B. thuringiensis spores, and heat inactivated B. thuringiensis spores. Heat inactivated spores were exposed to a temperature just high enough that no spores were observed to germinate. Elasticity values for the spore surfaces were determined by measuring the reflection and transmission of acoustic waves between a spore surface and an atomic force microscope (AFM) tip, assuming a Hertz contact model. B. thuringiensis spores had a higher and more variable elasticity then B. anthracis spores. Heat inactivation caused spore surface elasticity to decrease. Calculated average elasticities were 3.73 GPa for B. anthracis, 2.73 GPa for heat inactivated B. anthracis, 4.67 GPa for B. thuringiensis, and 3.57 GPa for heat inactivated B. thuringiensis.

15. SUBJECT TERMS

Bacillus anthracis, Spore, Heat Inactivation

16. SECURITY CLASSIFICATION OF:			17. LIMITATION OF ABSTRACT	18. NUMBER OF PAGES	19a. NAME OF RESPONSIBLE PERSON
a. REPORT	b. ABSTRACT	c. THIS PAGE		84	Dr. Larry W. Burggraf (ENP)
					19b. TELEPHONE NUMBER *(Include area code)* (937) 255-6565, ext 4507

Reset